

# A Study on The Dynamic Compressive Behaviors of Epoxy Adhesive Modified by Mixed Silica Micro-nanoparticles

(ミクロおよびナノサイズのシリカフィラーを充填したエポキシ接着剤の動特性に関する研究)

September, 2018

Yohanes

# Contents

Contents .....	i
Nomenclature .....	iii
Chapter 1 Introduction .....	1
1.1 Research background .....	1
1.2 Literature review .....	3
1.2.1 <i>The influences of adhesive properties on the joint performances</i> .....	3
1.2.2 <i>Stiffness and damping behaviors of neat epoxy adhesive</i> .....	3
1.2.3 <i>Silica-filled epoxy adhesive</i> .....	5
1.2.4 <i>Dynamic responses of epoxy/silica under high loading rate and elevated temperature</i> .....	8
1.3 Research problems .....	9
1.4 Objectives and approach .....	10
1.5 Summary .....	13
Chapter 2 Effects of mixed micro and nano silica particles on the dynamic compressive performances of epoxy adhesive .....	15
2.1 Introduction .....	15
2.2 Experimental method .....	18
2.2.1 <i>Materials and specimen preparations</i> .....	18
2.2.2 <i>Experimental apparatus and data validation</i> .....	20
2.2.3 <i>Stress-strain characteristic and stiffness estimation</i> .....	25
2.2.4 <i>Estimation of stress transmissibility and energy absorption</i> .....	27
2.3 Results and discussions on the effects of silica micro-nanoparticles to the dynamic stiffness and stress transmissibility of epoxy adhesive at the ambient temperature .....	29
2.4 Results and discussions on the effects of silica micro-nanoparticles on the dynamic responses of epoxy adhesive at the elevated temperature .....	32
2.4.1 <i>Effects of silica weight fraction</i> .....	33
2.4.2 <i>Effects of the composition ratio</i> .....	37
2.5 Conclusions .....	39
Chapter 3 Synergistic effects of mixed silica micro-nanoparticles on the compressive dynamic stiffness and damping of epoxy adhesive .....	41

3.1	Introduction .....	41
3.2	Experimental method.....	44
3.2.1	<i>Materials and specimen preparation</i> .....	45
3.2.2	<i>SHPB test apparatus</i> .....	46
3.2.3	<i>Calibration and data validity</i> .....	48
3.2.4	<i>Estimation of stiffness and damping</i> .....	51
3.3	Results and discussions.....	53
3.3.1	<i>Effects of silica micro-nanoparticles on dynamic stiffness</i> .....	56
3.3.2	<i>The synergistic effect of silica micro-nanoparticles on hysteretic damping</i> 62	
3.3.3	<i>Optimum composition ratio and weight fraction of silica micro-nanoparticles</i> .....	67
3.4	Conclusions.....	68
Chapter 4	Conclusions.....	70
4.1	The conclusions of the present studies .....	70
4.2	The outlook for future research.....	72
	Reference.....	73
	List of Publications.....	92
	Acknowledgments .....	93

## Nomenclature

$A_B$	The surface area of the pressure bar
$A_S$	The surface area of the specimen
$C_0$	Elastic wave speed in bar material
$E$	Dynamic stiffness of epoxy/silica
$E_0$	Dynamic stiffness of neat epoxy
$E_B$	Young's modulus of pressure bars
$E_\sigma$	Stress transmissibility
$E_R$	Impedance mismatch
$E_{Loss}$	The estimated loss of energy
$L$	Length of the striker bar
$L_S, D_S$	Length and diameter of the specimen, respectively
$P_1, P_2$	Compressive forces of the specimen at the interfaces of input bar-specimen and output bar-specimen, respectively
$T$	Temperature
$T_g$	Glass transition temperature
$T_L$	Loading pulse duration (duration of the incident pulse)
$v_{st}$	Impact speed of the striker bar
$v_1, v_2$	The velocity of the specimen at the interfaces of input bar-specimen and output bar-specimen, respectively
$\delta$	Hysteretic damping
$\varepsilon_t$	Incident pulse/incident strain wave

$\varepsilon_R$	Reflected pulse/reflected strain wave
$\varepsilon_T$	Transmitted pulse/transmitted strain wave
$ \varepsilon_I _{max}$	The amplitude of the incident strain wave
$ \varepsilon_R _{max}$	The amplitude of the reflected strain wave
$ \varepsilon_T _{max}$	The amplitude of the transmitted strain wave
$\dot{\varepsilon}_n$	Strain rate
$\varepsilon_n$	Strain
$\sigma_n$	Stress
$\Phi_{SP}$	Composition ratio of micro-nanoparticles

# Chapter 1

## Introduction

### 1.1 Research background

The use of structural adhesives is rising with the development of lightweight structures, such as aircraft and automobile. Structural adhesives facilitate the joints of dissimilar and composite materials, promote homogeneous stress distribution, minimize stress concentration, and provide a larger contact surface. They also avoid defects and changes in the material properties of the adherends, such as holes and heat affected zone produced by fastener and welding.

The epoxy-based adhesive is well-accepted for joint applications in industries owing to its beneficial natures. Compared to other adhesives, the epoxy is most lightweight, low in production cost, strong adhesion, good solvent (compatibility), curable in a wide range of temperature, highly resistant to heat, moisture, and chemicals. However, the epoxy adhesive is naturally brittle, vulnerable to crack initiation and growth, and sensitive to the loading rate and temperature. Particulate filler is introduced to minimize such drawbacks and improve mechanical responses of epoxy adhesive. Silica particle is commonly used to improve modulus and toughness which are essential for structural joints.

In practice, structural joints should endure various types of loadings under extreme environmental conditions, such as crushes, impacts, vibrations, extreme operational temperature ( $-50^{\circ}\text{C}$   $\sim 80^{\circ}\text{C}$ ), and corrosive environment. In such conditions, the structural adhesive should resist deformation and facilitate appropriate energy dissipation to maintain joint rigidity and reliability at a wide range of loading rates and temperatures. Therefore, experimental characterization of dynamic stiffness and damping of epoxy adhesive is critical for engineering design and analysis purposes. In the characterization, mixture variables of composite adhesives, e.g., filler/matrix ratio and multi-filler composition ratio, should be paid more attention to provide design options for the adhesive to match applications.

Up to date, stiffness and energy absorption behaviors of particulate-filled epoxy adhesive under various loading rates have been investigated by many researchers. They observed the mechanisms of stiffening and energy dissipation and the influencing variables. Section 1.2 introduces an overview of the progress and achievements of the previous works. Section 1.3 describes the research problems based on the overview of the previous works. Section 1.4 describes the objectives in this present study regarding the issues in section 1.3. Finally, a summary of this chapter is presented in section 1.5.

## 1.2 Literature review

### *1.2.1 The influences of adhesive properties on the joint performances*

Mechanical properties of structural adhesives affect the overall mechanical performances of structural joints. For instances, Higuchi et al. [1] reported that the increase of adherend/adhesive stiffness ratio increased the maximum principal stress at the interface of butt joints under impact tensile loadings. A similar study was conducted by Liao and Sawa [2] and demonstrated that the increase of adherend/adhesive stiffness ratio increased the normal stress. The more recent study was carried out by Hazimeh et al. [3] and showed that joint shear strength increased with the adhesive shear modulus. Asgharifar et al. [4] reported that stress transmissibility of bonded joints increased with the adhesive modulus. Such previous studies emphasized that the characterization of the adhesive properties is critical for structural joint design and analysis.

### *1.2.2 Stiffness and damping behaviors of neat epoxy adhesive*

The epoxy is one of the most used structural adhesives due to its high adhesion and compatibility with various types of materials. The epoxy polymer is viscoelastic in nature which are characterized by the storage modulus and the loss modulus. The storage modulus and the loss modulus measure the energy stored (stiffness) and dissipated (damping) during deformation, respectively. Such characteristics depend on the crosslinking density of epoxy which can be modified during the polymerization process [5–9]. For example, the densely cross-linked epoxy is brittle and exhibits high stiffness but low damping [10–13].



The stiffness and damping of epoxy are sensitive to the strain rate loadings. Increasing the strain rate enhances the modulus but reduces the damping of epoxy [14–20]. The increase in modulus and decrease in damping are the results of the epoxy embrittlement induced by the increase of loading rate [20,21]. The rate-sensitivities of modulus and damping depend on the epoxy natures and the loading conditions [22].

The damping performance depends on the deformation behaviors of epoxy. Under dynamic compressive loading, the epoxy exhibits elastic and viscoelastic-plastic deformation [15,16,23]. The hysteretic damping is indicated by stress-strain loop responses. The major energy dissipation occurred during nonlinear elastic (superelastic) deformation [23]. The epoxy deformation behaviors are also influenced by the strain rate. The epoxy exhibits ductile natures at low strain rate but changes to brittle at a high strain rate of compressive loadings [20,21] and thus, reduces the damping.

The stiffness of epoxy is also sensitive to the temperature owing to its inherent viscoelasticity. The epoxy stiffness decreases nonlinearly with the increase of temperature due to the increase in molecular mobility [17,24]. The rate-sensitivity of epoxy modulus also changes with temperature. The stiffness of epoxy is less sensitive to the strain rate at low temperature ( $-20^{\circ}\text{C}$ ) [18]. Thermal stability of adhesive stiffness and damping is of interest as the structures experience a wide range operating temperature.

To conclude the above paragraphs, despite the high performances in adhesion and power-to-weight ratio, neat epoxy is brittle and sensitive to loading rate and temperature. In practice, adhesive joints should resist deformation and dissipate energy in a wide range of loadings and temperatures. In this respect, the introduction of reinforcing particles to improve the desired properties of epoxy adhesive is necessary.

### *1.2.3 Silica-filled epoxy adhesive*

Silica particles are commonly used to stiffen epoxy adhesives owing to their rigidity. The modulus of epoxy/silica composite is determined by the composition ratio between the rigid particles and the soft epoxy matrix. The modulus increases with the increase of the content of silica particles in the composite space [25–43]. Mixture laws are used to predict the modulus of epoxy/silica at any particle content [41,44–46]. However, the discrepancy between the experimental results and the predicted modulus occurs frequently. Such discrepancy is attributed to the presence of the interphase which is formed by the matrix-filler interactions and has different properties to that of matrix and fillers [26,34].

The stiffness of interphase area depends on the matrix-filler interactions and the matrix adhesion [39]. Strong adhesion and good matrix-filler interfaces produce stiff interphase and hence, improve the overall modulus of epoxy composite [26,34,35,40,47]. In contrast, poor interfacial adhesion and matrix-filler interactions generate soft interphase and counteract the stiffening effect of silica particles [48–52]. The properties of the interphase were verified through nano-

indentation tests or estimated through a model [57,58]. Then, the more accurate prediction of composite modulus was obtained by including the interphase modulus in the constitutive model [34,54].

The stiffening effect of the interphase area is exploited by increasing particle contents or reducing particle sizes. However, a significant stiffening effect can be obtained only by varying particle sizes below the certain value [39]. In fact, nanoparticles increase the modulus more efficiently compared to microparticles at a given weight fraction owing to the larger specific surface area. Nonetheless, the modulus of epoxy/nanosilica frequently underperforms the predicted value owing to the mixing problems. Poor mixing of matrix and nanoparticles creates holes, cavities, and aggregates/agglomerates which reduce the stiffening effect of silica particles on the composite [55,56].

Well-dispersion is required to form large and continuous interphase area in the composites and thus, to exploit the exponential stiffening effect of silica nanoparticle. However, without any treatment silica particles tend to cluster during mixing and reduce the stiffening effect [57,58]. Conventional mechanical mixers generate a limited shear force to break a high number of nanoparticle colonies. For example, Bondioli et al. [34] observed that aggregation of silica nanoparticle was initiated at 5-wt.%. Sol-gel technique, ultrasonication, mild processing, and silica surface treatment were used to prevent and minimize aggregate/agglomerate [40,59–61]. However, such techniques are complicated and less effective in cost and time to prepare particulate-filled epoxy.

Composing particles of different sizes (bimodal) reduce viscosity and prevent agglomeration during mixing [58,62–64]. The large particle breaks agglomerates into smaller aggregates and improves particle distribution. The dispersion quality of bimodal particles depends on the composition ratio and the size ratio of large-to-small particles and the absolute size of particles [58,62–64]. This alternative technique is simpler and more efficient compared to the previously mentioned techniques.

Synergetic effects were expected from two-size silica particles to improve the epoxy performances. Kwon et al. [65] and Dittanet and Pearson [31] mixed silica micro-nanoparticles in various size ratios to modify the epoxy properties. They found that variations of particle sizes and composition ratios slightly affect the modulus but significantly affect the toughness. They found that two-size particles generate synergetic toughening by dissipating more energy via complex interactions of matrix-filler and interparticle. Shariati et al. [66] composed two-size silica nanoparticles but did not find any significant effect on modulus nor energy absorption. More recently, Keivani et al. [67] used micro-nanoparticles to reinforce epoxy and found that the modulus increases monotonically with increasing the portion of silica nanoparticles. Dorigato et al. [68] and Dzenis [69] reported that aggregated nanoparticles provide an additional stiffening effect on the epoxy by trapping some matrices within the strong aggregates. They proposed a model to explain the new reinforcing mechanism induced by particle aggregation.

Stress concentration induced by silica particles produces high shear and normal strains that promote significant viscoelastic energy loss [70]. The inclusion of silica nanoparticles preserves the ductility of epoxy. The improved ductility indicates the presence of additional energy dissipation mechanisms induced by nanoparticles [33]. There are several mechanisms of energy dissipation induced by matrix-nanoparticle interactions such as matrix shear bandings [32], local plastic deformations [40], and particles debonding [71].

In the previous studies, the synergistic effects of silica micro-nanoparticles on the stiffness and damping of epoxy under dynamic loads had not been investigated. The reinforcing mechanisms of the epoxy adhesive filled with two-size silica particles are still unexplained. Epoxy natures, matrix-filler interactions, and aggregation must be investigated under dynamic loadings.

#### *1.2.4 Dynamic responses of epoxy/silica under high loading rate and elevated temperature*

The stiffness and damping of epoxy/silica are sensitive to strain rate due to viscoelastic natures of the epoxy matrix. Dynamic compressive moduli of epoxy/silica increase with increasing strain rate and the content of silica particles [48,72,73]. However, the damping decreases with the increase of particle content and size owing to the reduced ductility. The decrease of ductility is caused by the stress concentration induced by agglomerated particles and the decreased polymer mobility which unable to catch up the instant strain generated at high strain rate.

Kwon et al. [74] used bimodal micro-nanoparticle to reinforced epoxy and investigated the thermal stability of epoxy/silica. They found that the stiffness of the composite increased with the portion of silica nanoparticles regardless of the temperature. It was noticed that the effect of micro-nanoparticle composition ratio on the stiffness was decreased with increasing temperature and was negligible near glass transition temperature ( $T_g$ ). Nonetheless, the effect of micro-nanoparticles on the epoxy under impact and elevated temperature are rarely studied.

### 1.3 Research problems

The preceding section overviewed previous studies which are related to the characterizations of the epoxy adhesive. Based on that overview, there are several issues to notice as follows:

- 1) The effect of mono-size silica particles on the modulus and toughness of epoxy adhesive under both quasi-static and dynamic loadings had been studied intensively. However, the effects of two-size particles on the mechanical responses of epoxy adhesive had not been investigated sufficiently, especially under dynamic loads. Therefore, the reinforcing effects of silica micro-nanoparticles remain unclear.
- 2) The effect of silica particles on the toughness of epoxy was explored immensely. However, the hysteretic damping behaviors of epoxy adhesive had been barely studied, particularly for the epoxy reinforced by silica micro-

nanoparticles. Hysteretic damping is a critical property of adhesive to response small strain dynamic loadings such as impact and vibration.

- 3) In the interest of thermal stability of epoxy adhesive, the effect of temperature on the mechanical responses of epoxy and epoxy/silica had been investigated in the previous studies. However, the thermal stability of epoxy modified by silica micro-nanoparticles under dynamic loadings has been paid little attention.

Based on the overlooked issues in the previous study, in the present study, we focus on the following issues:

- 1) The effects of composition ratio and weight of silica micro-nanoparticles on the dynamic performances of bulk epoxy adhesive under impact loadings.
- 2) The effect of temperature on the dynamic performances of epoxy modified by silica micro-nanoparticles under impact loadings.
- 3) The effectivity of two-size particles to improve particle dispersion and to generate the subsequent synergistic effects on the epoxy adhesive.

## 1.4 Objectives and approach

Regarding the evaluation of the issues presented in the previous section, the objectives of the present study are described as follows:

- 1) To obtain the stress-strain loop responses of the epoxy adhesive modified by silica micro-nanoparticles and to estimate the dynamic stiffness and hysteretic damping under impact loadings.
- 2) To evaluate the effects of composition ratio and weight fraction of silica micro-nanoparticles on the dynamic responses of epoxy adhesive and to observe the possible synergistic effects generated by micro-nanoparticles.
- 3) To evaluate the reinforcing performances of silica micro-nanoparticles on the dynamic responses of epoxy adhesive at the elevated temperature.

The contributions of this present study are:

- 1) To fill the gap of knowledge on the dynamic responses of epoxy adhesive modified with silica micro-nanoparticles under impact loadings, which are overlooked in the previous studies. Continuous data on the epoxy adhesive performance from quasi-static to high strain rate loadings are necessary for structural design and analysis.
- 2) To measure the effectiveness and the limitations of two-size silica particles to improve particles dispersion using a conventional mixer and the subsequent synergistic effects on the epoxy adhesive.
- 3) To provide design options or guidelines for modifying the dynamic performances of epoxy adhesive by choosing an appropriate composition ratio and weight fraction of silica micro-nanoparticles to match certain applications.



- 4) To find the optimum composition ratio of silica micro-nanoparticles that maximizes the stiffness and damping performances of epoxy adhesive.

The detail of the contents is introduced as follows:

In Chapter 2 [**Effects of mixed micro and nano silica particles on the dynamic compressive performances of epoxy adhesive**], the split Hopkinson pressure bar (SHPB) apparatus was used to evaluate the effects of silica micro-nanoparticles on the dynamic modulus, stress transmissibility, and loss energy of epoxy adhesive at the elevated temperature. The limitations of the present SHPB technique to produce smooth and closed-loop stress-strain responses are discussed. A less-fluctuating stress-strain loop is necessary to estimate hysteretic damping accurately. In the absence of smooth stress-strain loops, a new parameter to measure the energy absorption performance was introduced. The dynamic stiffness, stress transmissibility, and energy loss performances are evaluated for different composition ratios and weight fractions of 5-wt.% and 10-wt.% silica micro-nanoparticles. The stiffening effect of silica micro-nanoparticles at the elevated temperature is evaluated. The trade-off between dynamic stiffness and energy loss are discussed. Finally, the optimum composition ratio of silica micro-nanoparticle that maximizes the energy loss while preserving the stiffness was presented.

In Chapter 3 [**Synergistic effects of silica mixed micro and nanoparticles on the stiffness and damping of epoxy adhesives**], the SHPB test was modified to obtain smooth stress-strain loop responses of the materials by using bonded specimen instead of the sandwiched specimen. The validity and reliability, as well

as the limitations of the modified technique, are discussed. The dynamic stiffness and hysteretic damping are evaluated for the various composition ratios at increasing particle content of 2-wt.%, 5-wt.%, and 10-wt.%. The synergetic effects of silica micro-nanoparticles are discussed in terms of the contribution of the interphase area. The effectiveness of two-size particles to improve particle dispersion is also discussed. The mechanism of energy dissipation via damages is presented. Finally, the optimum composition ratio of micro-nanoparticle which maximizes both stiffness and damping is presented.

In Chapter 4 [**Conclusions**], the effects of silica micro-nanoparticles on the dynamic responses of bulk epoxy adhesive were summarized based on the results of Chapters 2 and 3. Furthermore, the outlooks for the future study in correlation with the topic in the present study were described.

## 1.5 Summary

In this chapter, the research topic about the effects of silica micro-nanoparticles on the dynamic responses of bulk epoxy adhesive is introduced. Previous studies related to this topic are overviewed to recognize the achievements, to develop motivations, and to describe the necessities and the objectives of the present study, which are described as follows:

- 1) The dynamic responses of the epoxy modified by silica micro-nanoparticles under impact loadings had not been investigated in the previous studies.

- 2) The effects of composition ratio and silica weight fraction of silica particles on the dynamic stiffness and hysteretic damping of epoxy adhesive should be examined.
- 3) The reinforcing effect of silica micro-nanoparticles on the dynamic responses of epoxy adhesive at the temperature near the glass transition temperature of the epoxy ( $T_g=55^\circ\text{C}$ ) under impact loads had not been evaluated.

## Chapter 2

# Effects of mixed micro and nano silica particles on the dynamic compressive performances of epoxy adhesive

### 2.1 Introduction

Epoxy is widely used both as adhesives and composites in industrial and structural applications due to its superiority in strength to weight ratio. Understanding the stiffness behavior of epoxy at various strain rate is critical for design and analysis purposes. Stiffness behavior is required to estimate the response of structures subjected to dynamic loads such as impact and shock. The stiffness of epoxy composite depends on the inherent characteristics of its constituent materials and their interactions.

Silica particles are commonly used to enhance the epoxy stiffness due to their high modulus and strong adhesion with the epoxy matrix. Strong adhesion of epoxy-silica restricts molecular mobility and deformation of the epoxy matrix at the interphase area. The interphase area, which is stronger than the matrix, facilitates higher load transfer between the epoxy matrix and silica particles and thus enhances the epoxy stiffness. The interphase area can be increased by increasing the content

of silica particles in the epoxy for a given particle size or reducing the size of silica particles for a given weight fraction. Reducing the size of silica particles into nano-scale effectively improves the stiffness of epoxy because it avoids stress concentration induced by larger size silica particles (i.e., micro silica particle) [26,32,39,40,88–90].

Nano silica particles must be well-dispersed in the epoxy matrix to effectively increase the stiffness of epoxy [39]. However, without any surface modification, high content of nano silica particles tend to aggregate or agglomerate in the epoxy which influences the mechanical properties of the epoxy adhesive [68], [78]. Moreover, nano silica particles tend to increase the viscosity of the epoxy which causes difficulties in the mixing process. Agglomeration of the nanoparticles can be prevented by introducing larger size particles, such as microparticles, into the mixture. However, the references investigated the influence of two-size silica particles on the stiffness of epoxy are very limited.

The influence of two-size silica particles on the stiffness of epoxy has been reported to depend on the size ratio of two particles. Kwon et al. [65] and Adachi et al., [79] using relatively small size ratio of silica fillers (i.e., 1.56 and 0.24  $\mu\text{m}$  in diameters), have reported that the composition ratio slightly influences the bending stiffness and static tensile stiffness. However, they found that the epoxy stiffness strongly depends on the weight fraction of the silica particles. More recently, using larger size ratio (i.e., 42  $\mu\text{m}$  and 23, 74, 174 nm in diameters), Dittanet et al. [31], showed that the composition ratio of two sizes of silica particles significantly

influenced the static tensile stiffness of epoxy. They reported that the nanoparticles around microparticles induced stress concentration that weakened the bonding strength between epoxy and micro silica. Weak bonding reduces load transfer from matrix to particles and thus, reduces the stiffness. However, even though the effect of two sizes of silica particles on the static stiffness of epoxy using different size ratio were investigated, little attention has been paid to stiffness behavior of epoxy filled with micro and nano silica particle subjected to high strain rate loadings.

In the previous works, the investigations of stiffness behavior of epoxy at high strain rate loading have been limited. High strain rate loading restricts the molecular mobility of the epoxy matrix and results in a stiffer response [20,80–84]. In opposite, the molecular mobility increases with the temperature [20]. Due to strong adhesion of silica/epoxy, molecular mobility of the epoxy matrix is more restricted as silica particles were introduced, and thus increases the dynamic stiffness. Dynamic stiffness exhibits significant dependence on the size of silica particles and increases as the size of silica particles reduced into nanoscale [20]. The dynamic stiffness is also influenced by the weight fraction and distribution of silica particles in the epoxy matrix [20,72,80,84,85]. Moreover, dynamic stiffness performance of epoxy is sensitive to the temperature which influences the molecular mobility of the epoxy. However, it is important to note that, due to the complicated interaction between filler and matrix, the influence of mixed micro and nano silica particles on the stiffness at high strain rate has been paid little attention. Therefore, the present research contribution is to fill this gap of knowledge and to provide experimental evidence for practical implementation. By knowing the

influence of mixed micro and nano silica particles on the dynamic stiffness behavior of epoxy adhesive, it is possible to design its stiffness performance for appropriate applications.

The present chapter investigates the dynamic stiffness dependency on the composition ratio of micro and nano silica particle as well as silica weight fraction at the elevated temperature by means of split Hopkinson pressure bars (SHPB). Stress transmissibility and energy absorption are also observed as extended performance parameters.

## 2.2 Experimental method

### 2.2.1 *Materials and specimen preparations*

The specimens were made from epoxy adhesive, Scotch-Weld 1838 branded by 3M™. The neat epoxy has a glass transition temperature ( $T_g$ ) of 55°C at which the epoxy natures change from the glassy state to the rubbery state. The epoxy was filled with micro and nano silica particles without any surface modification. Micro and nano silica are 74 GPa of Young's Modulus, 17  $\mu\text{m}$  and 34nm in diameters, and with 3.4  $\text{m}^2/\text{g}$  and 80  $\text{m}^2/\text{g}$  in specific surface areas, respectively. Micro and nano silica particles were mixed with the epoxy adhesive sequentially using a planetary centrifugal mixer (Thinky AR-100). Each size of particles was mixed in an appropriate time to obtain a visually homogeneous mixture and followed by degassing process to avoid bubbles. The mixture was poured into the prepared mold with care, pressed to produce porosity-free

cylindrical specimens, as shown in Fig. 2-1, and cured for 24 hours. The specimens were 16 mm in diameter ( $D_S$ ) and were smaller than the pressure bars to maintain their full contact surfaces during loading. The specimen ratio of thickness to diameter,  $L_S/D_S = 0.5$ , was introduced to avoid the inertia effect in the measurement. The total weight fractions of mixed micro and nano silica particles in the epoxy adhesive were 5 wt.% and 10 wt.% with the composition ratio listed in Tabel 2-1.

Table 2-1 Composition ratio of silica micro-nanoparticles

Mixture ratio, $\Phi_{SP}$	Silica particle diameter	
	34 $\mu\text{m}$	17 nm
0% (pure microparticle)	100%	0%
25%	75%	25%
50%	50%	50%
75%	25%	75%
100% (pure nanoparticle)	0%	100%

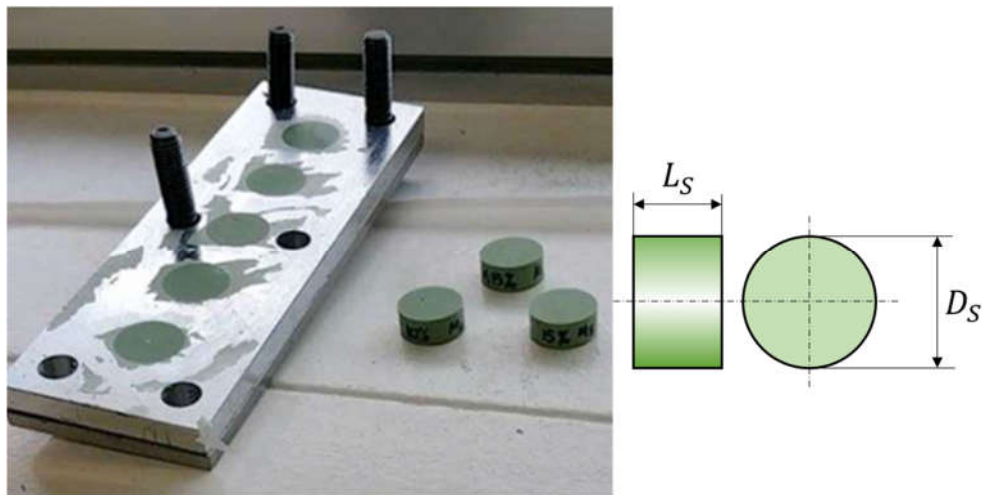


Fig. 2-1 The cured specimen and mold for SHPB test



### 2.2.2 Experimental apparatus and data validation

The split Hopkinson pressure bar (SHPB) test rig used in the present work consists of a striker bar, input and output pressure bars, strain gauges (KYOWA KFG-2-120-C1-11L5M3R), strain transducers (KYOWA DB-120A) with signal conditioners (KYOWA CDV-900A), and a digital oscilloscope (IWATSU DS-5102) for data recording as shown in Fig. 2-2. The SHPB was designed by considering the assumption of one-dimensional stress wave propagation which is required to derive the stress-strain equations. All bars were made of stainless steel, 20 mm in diameter, Young's modulus of 209 GPa, density of 8750 kg/m<sup>3</sup>, and Poisson ratio of 0.3. Both input and output pressure bars were identical of 2000 mm in length. The crowned striker bar of 300 mm in length ( $L$ ) was propelled as a pendulum to generate  $140 \pm 5 \text{ s}^{-1}$  strain rate and  $\pm 200 \text{ }\mu\text{s}$  duration of the incident pulse as it stroked the input bar. The loading duration ( $T_L$ ) and the amplitude ( $|\varepsilon_I|_{max}$ ) of the incident pulse were calculated using Eqs. (2-1) and (2-2), accordingly,

$$T_L = \frac{2L}{C_0} \quad (2 - 1)$$

$$|\varepsilon_I|_{max} = \frac{1}{2} \frac{v_{st}}{C_0} \quad (2 - 2)$$

where  $v_{st}$  is the impact speed of striker bar, and  $C_0$  is the elastic wave speed in the input bar. The results were used to plot the Lagrangian diagram as shown in Fig. 2-3 and to locate the strain gauges on the bars. The crowned impact face, which is adopted from Yokoyama et al. [15,16,23], was used to extend the rise time of the

incident pulse and thus, modify the pulse shape. The Fast Fourier Transform (FFT) technique was applied to compensate the signal fluctuations induced by wave dispersion as adopted from Zhao and Gary [86].

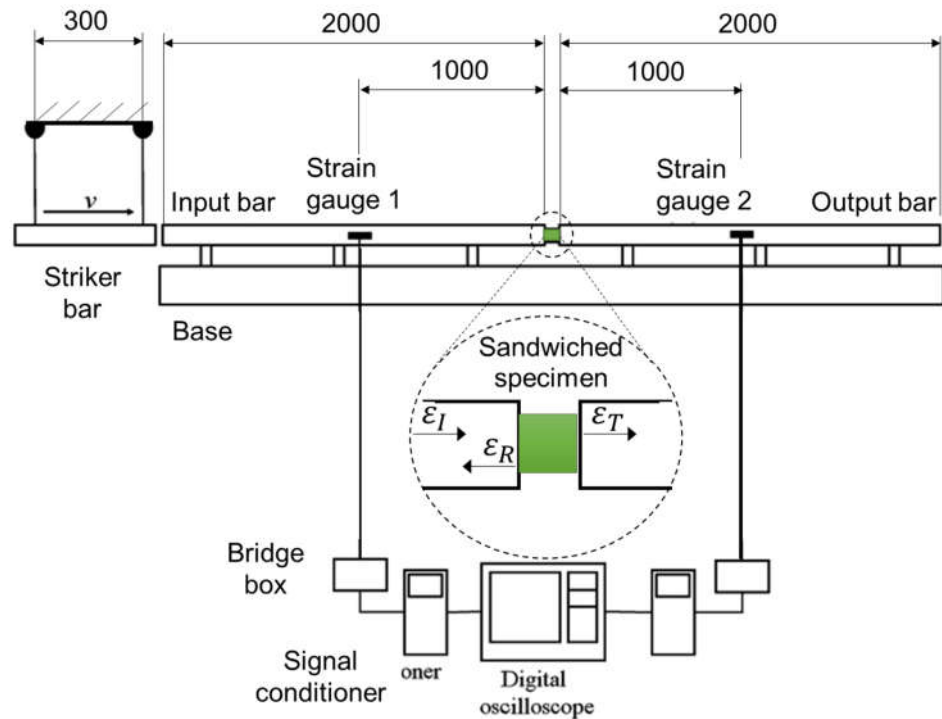


**Fig. 2-2** A schematic of the split Hopkinson pressure bar apparatus (all dimensions are in mm)

The generated incident pulse ( $\epsilon_I$ ) travels through the input bar to the specimen which is sandwiched between both pressure bars. Due to impedance mismatch at the interface of the input bar and the specimen, some part of the pulse is reflected ( $\epsilon_R$ ) to the input bar while the other part is transmitted ( $\epsilon_T$ ) to the output bar (Fig. 2-2). Incident and reflected pulses are measured at the input bar while the transmitted pulse is measured at the output bar using strain gauges. The strain

gauges were located at the middle of both pressure bars purposely to avoid signal overlap, based on Lagrangian diagram as shown in Fig. 2-3.

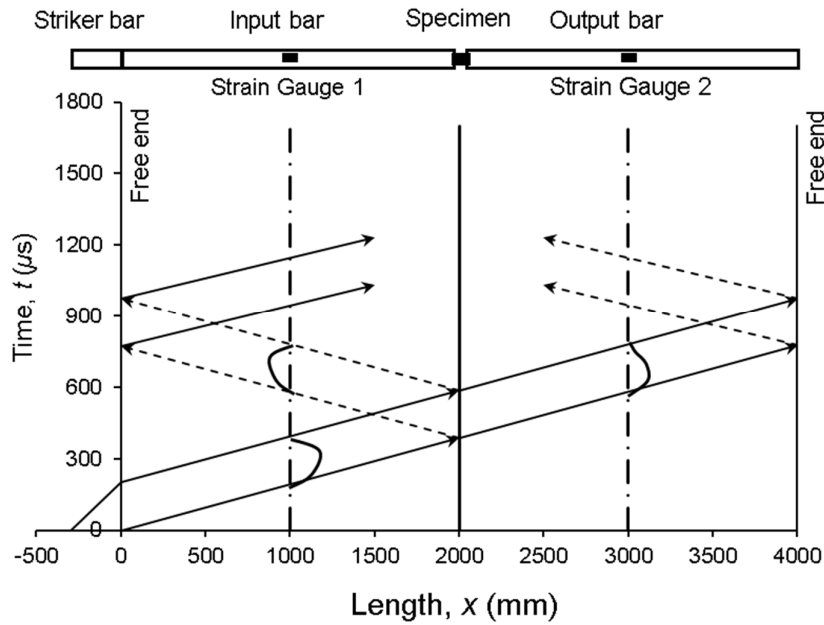


**Fig. 2-3** Lagrangian diagram to locate the strain gauges in which avoid signal overlap.

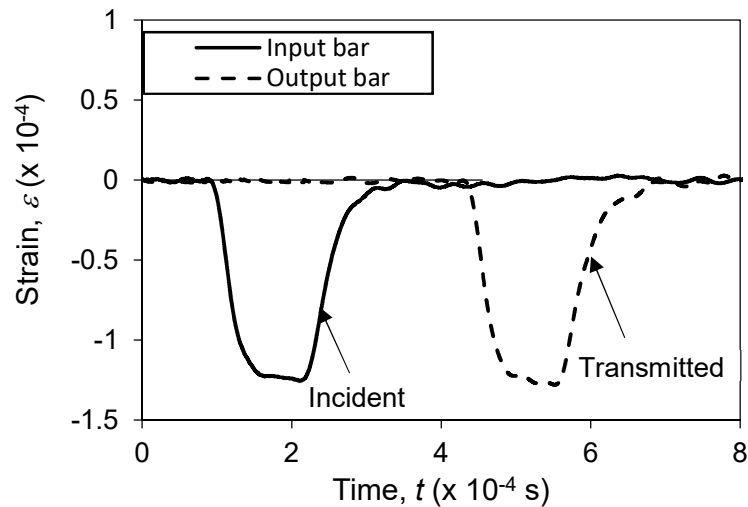


**Fig. 2-4** Recorded signal of bar alignment. Nearly identical pulses of the incident and transmitted, and the absence of reflected pulse confirmed that the bar system is in good alignment.

The SHPB system was calibrated before the measurement to ensure its validity and accuracy. First, the striker bar impacted the pressure bars without specimen sandwiched between them. The interface of pressure bars was lubricated to minimize the friction; thus, the bar system can be considered as a single bar. As can be observed in Fig. 2-4, the transmitted pulse is identical to the incident pulse in its shape, amplitude, and duration. No reflected pulse caused by impedance mismatch is found in this calibration test which means the pressure bars are correctly aligned. By this measurement condition, the reflected pulse found in the specimen test as shown in Fig. 2-5 is contributed by the sandwiched specimen only. Therefore, the measurement condition is valid to obtain data from the specimen and the test system.

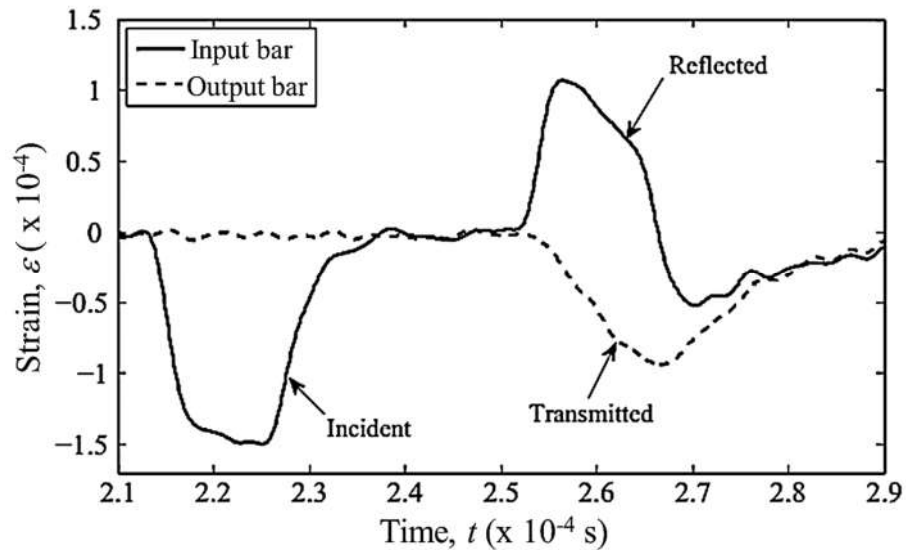


**Fig. 2-5** A typically measured signals of strain waves on the pressure bars with specimen attached.

Second, the dynamic equilibrium condition at the specimen was verified during compressive loading. Dynamic equilibrium is obtained when the compressive loads  $P_1$  and  $P_2$  at both specimen surfaces are equal. The compressive loads are described as follows

$$P_1 = A_B E_B \{\varepsilon_L(t) + \varepsilon_R(t)\} \quad (2-3)$$

$$P_2 = A_B E_B \varepsilon_T(t) \quad (2-4)$$

where  $A_B$  is cross-sectional area of the bars,  $E_B$  is Young's modulus of the bars. The compressive loads, as observed in Fig. 2-6, are similar and overlapped which means the dynamic equilibrium condition is obtained. Therefore, the influence of friction between the bars and the specimen on the SHPB system used in the present experiments can be ignored and the accuracy of the obtained data is verified.

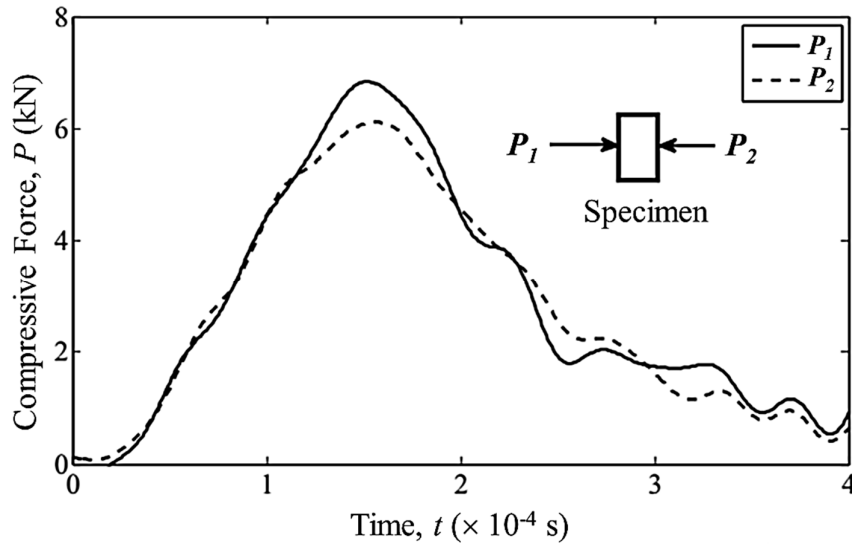


**Fig. 2-6** Dynamic equilibrium in the specimen was verified by the nearly overlapped compressive forces at both ends of the specimen

### 2.2.3 Stress-strain characteristic and stiffness estimation

Once the measurement condition had been verified for its validity and accuracy, strain rate history and stress-strain curve can be obtained from the measured strain waves using the following equations:

$$\sigma_n = \frac{A_B}{A_S} E_B \varepsilon_T(t) \quad (2 - 5)$$

$$\dot{\varepsilon}_n = \frac{2C_0}{L_S} \varepsilon_R(t) \quad (2 - 6)$$

$$\varepsilon_n = \frac{2C_0}{L_S} \int \varepsilon_R(t) dt \quad (2 - 7)$$

where,  $\sigma_n$  is the stress,  $\varepsilon_n$  is the strain,  $L_S$  and  $A_S$  are the thickness and the cross-sectional area of the specimen, respectively, and  $t$  is time duration. Strain rate time history and stress-strain curves obtained from the calculation are shown in Figs. 2-7 and 2-8, respectively. The strain rate time history and the stress-strain curve show that specimen, due to the low impact load, underwent compressive elastic deformation only.

In the ideal measurement, the working strain rate should be constant during loading. However, this ideal condition is practically difficult to obtain. In the present research, strain rate always changes during loading as shown in Fig. 2-7. Specimen was compressed for the first 170  $\mu s$  loading time then released to its original shape for the remaining loading time. However, during compressive loading, constant strain rate occurred for a short time near its maximum point.

Therefore, in the present research, the strain rate was estimated at its maximum point.

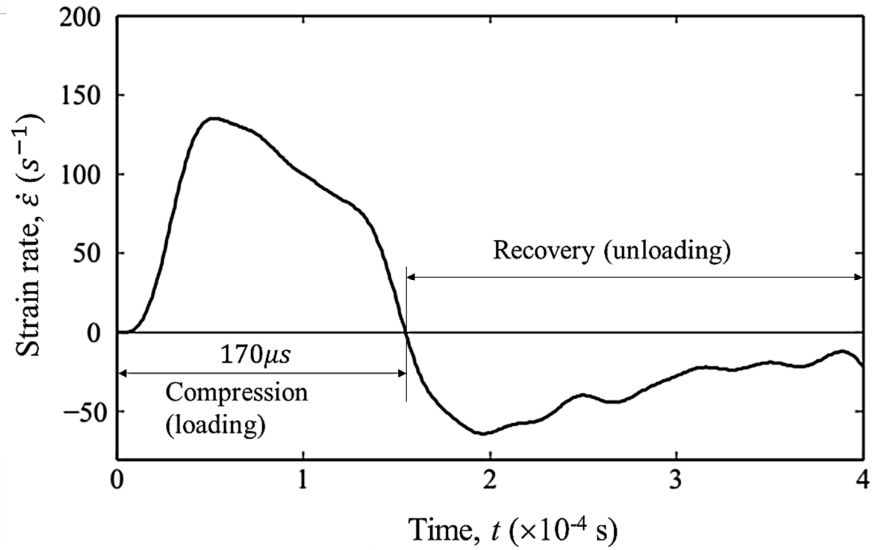


Fig. 2-7 Strain rate history in the specimen for a typical measurement.

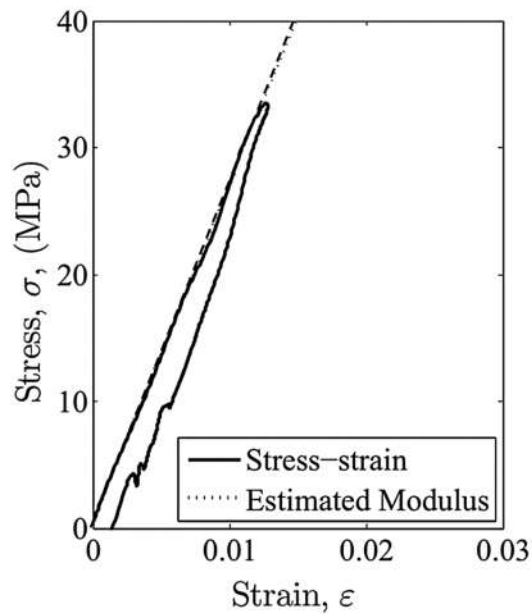
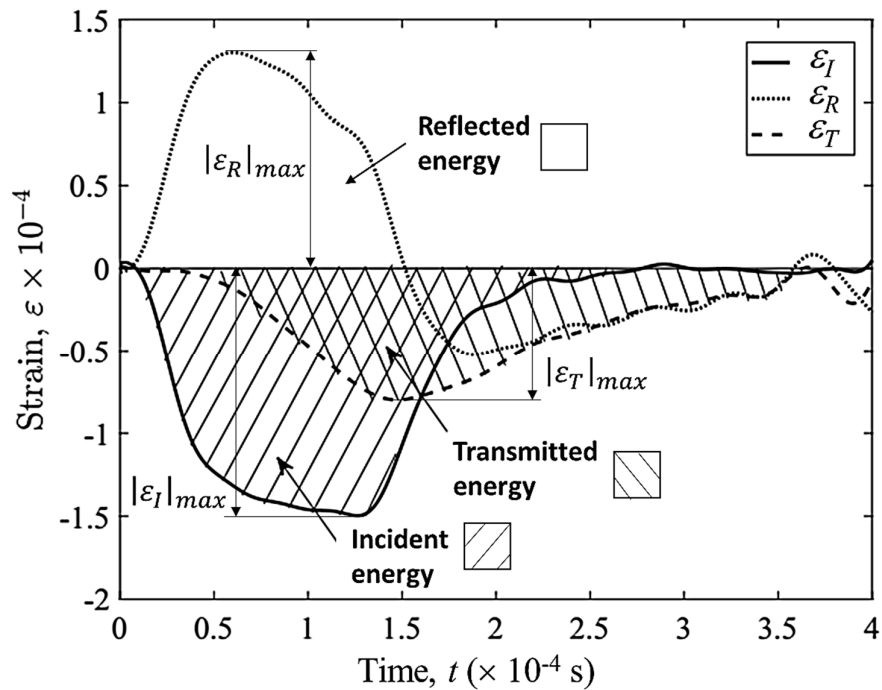


Fig. 2-8 Stress-strain response and estimated modulus of a typical measurement

The dynamic stiffness of specimen is represented by its modulus which is estimated from the initial slope of stress-strain curve as shown in Fig. 2-8. Due to low impact loading, only the elastic region was obtained from the measurement. Therefore, yielding strength and failure strength were not found in the stress-strain curve. However, this elastic region of stress-strain curve is appropriate for stiffness estimation.



**Fig. 2-9** The hatched pulse area represents the strain energy in the specimen

#### 2.2.4 Estimation of stress transmissibility and energy absorption

In the present chapter, two approaches were used to define the stress transmissibility ( $E_\sigma$ ). First, considering the strain pulses as a representative measure of load, the stress transmissibility was defined as the amplitude of transmitted pulse



(Fig. 2-9). Second, considering the area covered by the pulses as the representative measure of energy, the stress transmissibility was defined as the area covered by the transmitted pulse (Fig. 2-9). The measures of load and energy of the transmitted pulse were normalized by those of the incident pulse, respectively, to compare the result of each test. These definitions of the stress transmissibility were formulated in the Eqs. (2-8.a) and (2-8.b), respectively. Using the first approach, the impedance mismatch ( $E_R$ ) between the input bar and the specimen was defined as the amplitude of the reflected pulse as described by the Eqs. (2-9).

$$E_{\sigma} = \frac{|\varepsilon_T|_{max}}{|\varepsilon_I|_{max}} \times 100\% \quad (2 - 8. a)$$

$$E_{\sigma} = \left( \int \varepsilon_T dt / \int \varepsilon_I dt \right) \times 100\% \quad (2 - 8. b)$$

$$E_R = \frac{|\varepsilon_R|_{max}}{|\varepsilon_I|_{max}} \times 100\% \quad (2 - 9)$$

The hysteretic damping was difficult to be computed owing to the incomplete and fluctuated stress-strain response during specimen recovery (unloading) for most of the tests. The main reason for this problem was due to small strain applied and improper specimen contact during unloading. Therefore, considering the pulse area as a representative measure of energy previously mentioned, the damping was estimated by the difference of the area of the strain pulses at the input bar with the area of the strain pulse at the output bar. Then, by ignoring energy loss through wave dispersion, the damping was formulated as the

Eq. (2-10). Although this equation does not quantify the hysteretic damping, it facilitates us to qualitatively compare the energy loss for each test condition.

$$E_{Loss} = \left( \int (\varepsilon_I + \varepsilon_R - \varepsilon_T) dt / \int \varepsilon_I dt \right) \times 100\% \quad (2 - 10)$$

### 2.3 Results and discussions on the effects of silica micro-nanoparticles to the dynamic stiffness and stress transmissibility of epoxy adhesive at the ambient temperature

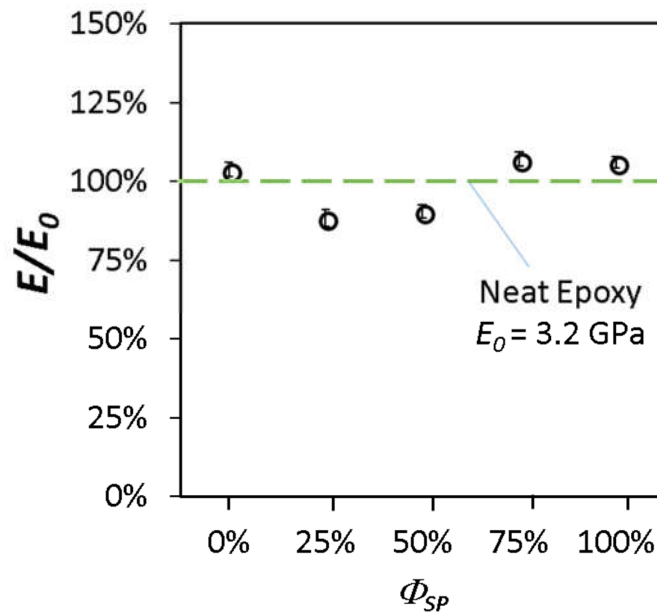


**Fig. 2-10** The effect of particle composition ratio on the dynamic stiffness of epoxy adhesive at 5-wt.% silica micro-nanoparticles

This section describes the effect of the composition ratio of 5-wt.% silica micro-nanoparticles on the dynamic stiffness and stress transmissibility of the epoxy adhesive at the ambient temperature as mentioned at the early of this chapter.

The effect of the composition ratio of 5-wt.% silica micro-nanoparticles on the dynamic modulus of epoxy is shown in Fig. 2-10. The dynamic modulus of silica-filled epoxy is represented relative to that of neat epoxy ( $E/E_0$ ) to highlight the stiffening effect of silica particles. The dynamic modulus of neat epoxy obtained from the measurement was 3.2 GPa. The deviation of each specimen was less than 5%. Dynamic stiffness of silica-filled epoxy varied nonmonotonically with the particle composition ratio. A slight enhancement of dynamic modulus was obtained by addition of silica microparticle ( $\Phi_{SP} = 0\%$ ). Then, the dynamic modulus decreased lower than that of neat epoxy as the silica nanoparticles presence ( $\Phi_{SP} = 25\%$  and  $50\%$ ). However, maximum stiffness was obtained at a composition ratio of 75% nanoparticles and 25% microparticles ( $\Phi_{SP} = 75\%$ ).

The addition 5wt.% of pure silica microparticle ( $\Phi_{SP} = 0\%$ ) marginally increased the dynamic modulus ( $E/E_0 = 104\%$ ). This small enhancement might be due to low particles content. In the previous work, Owens and Tippur [73] obtained similar results. They found that the dynamic modulus increases with the particles volume fraction. However, in the present work, the composition ratio of 75% ( $\Phi_{SP} = 75\%$ ) results in a remarkable increase of dynamic modulus ( $E/E_0 = 107\%$ ) at a given weight fraction (5-wt.%). These results suggest that the stronger stiffening effect promoted by nanoparticles is resulted from the larger interphase area provided.

The presence of nanoparticles at  $\Phi_{SP} = 25\%$  and  $50\%$ , however, counteract the stiffening effect of silica particles. There are several possible reasons related to

such softening effect. First, microparticles might introduce high-stress concentration factor and create damage and thus, reduce the stiffness. Second, highly dispersed nanoparticles might shift the glass transition temperature and result in lower stiffness. However, the fact that composition ratio of higher nanoparticle content ( $\Phi_{SP} = 75\%$ ) results in higher stiffness negates the second reason. Third, agglomeration of nanoparticles during mixing weakens the matrix-filler interaction. Agglomerates are very fragile to impact and thus, reduces the overall dynamic stiffness of epoxy composites. Moreover, the clustered particles might prevent perfect crosslinking of epoxy and result in a softer matrix. SEM analysis should be conducted to verify the existence of agglomerates. However, it is challenging to observe the microstructure owing to the large difference of particle sizes, i.e., microparticle vs. nanoparticle.

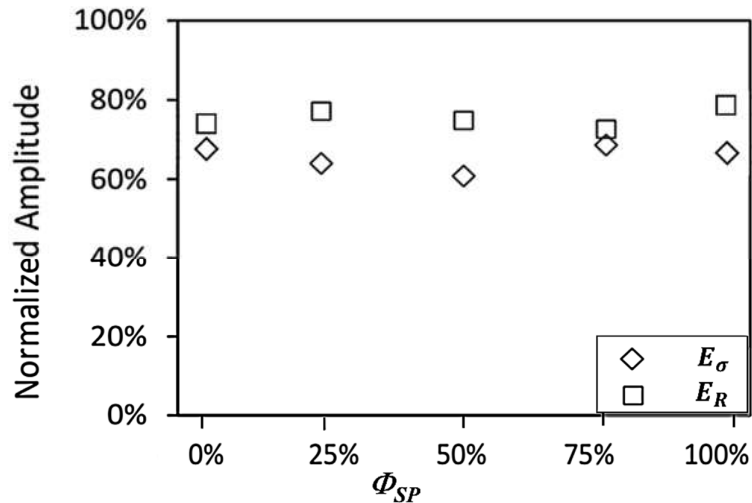


**Fig. 2-11** The effect of particle composition ratio on the stress transmissibility and impedance mismatch according to the Eqs. (2-8.a) and (2-9.a).

The stress transmissibility performance and the impedance mismatch of each specimen, based on the Eqs. (2-8.a) and (2-9.a) are represented by Fig. 2-11. Stress transmissibility ( $E_\sigma$ ) varied nonmonotonically with the particle composition ratio in the similar tendency with dynamic modulus while the impedance mismatch ( $E_R$ ) is in the opposite. The increased modulus facilitates a higher energy transmitted through the specimen and thus, reduces the portion of energy reflected due to impedance mismatch.

## 2.4 Results and discussions on the effects of silica micro-nanoparticles on the dynamic responses of epoxy adhesive at the elevated temperature

The influences of two-size silica particles on the dynamic stiffness of epoxy were investigated using the SHPB. The dynamic stiffness was estimated from the stress-strain curve obtained from the measured strain waves. The dynamic stiffness dependence on the composition ratio and the weight fraction of silica particles at different temperatures are presented in Fig. 2-12. The composition ratio, varied from pure micro silica ( $\Phi_{SP} = 0\%$ ) to pure nano silica ( $\Phi_{SP} = 100\%$ ), are represented by the horizontal axis. To measure the influence of silica particles on the epoxy, the dynamic stiffness of epoxy/silica composite is compared with the that of neat epoxy which is represented by the dashed line. The dynamic stiffness was firmly influenced by both the composition ratio and the weight fraction at the room temperature (Fig. 2-12.a). However, the influence decreased and became less significant as the temperature approached to  $T_g$  (Fig. 2-12.c). Therefore, the dependency of the stress transmissibility and the loss energy performance were

evaluated at room temperature only as shown in Figs. 2-13 and 2-14, respectively. The influence of the composition ratio and the weight fraction of the silica particles on the dynamic stiffness, stress transmissibility, and loss energy performance will be discussed in the following section.

Deviations were found in the estimated dynamic stiffness, stress transmissibility, and loss energy performances. The deviations were mainly caused by the variation in the mixing process of specimens and the included noises in the measurement which distorted the shape of strain waves. The effect of specimen variations caused by mixing process on the deviations of data was minimized by using five samples for each variable in the weight fraction and composition ratio. The distorted strain waves influenced the obtained stress-strain curves and thus, resulted in the deviations of the estimated dynamic stiffness (Fig. 2-12).

#### *2.4.1 Effects of silica weight fraction*

In the previous work, the influence of pure nano silica particle on the dynamic stiffness of epoxy had been investigated by Ma et al. [84]. It reported that the dynamic stiffness increased with the weight fraction of silica particles. In the present work, mixed micro and nano silica particles were used to reinforce the epoxy adhesive. Regardless the size and the composition of silica particles, enhancement on the dynamic stiffness of epoxy due to the increase of silica weight fraction was also observed (Figs. 2-12.a and b). The epoxy/silica interphase area was increased by silica weight fraction which induced more restriction to the

mobility of the epoxy matrix at the interphase and thus, resulted in stiffer epoxy/silica composite.

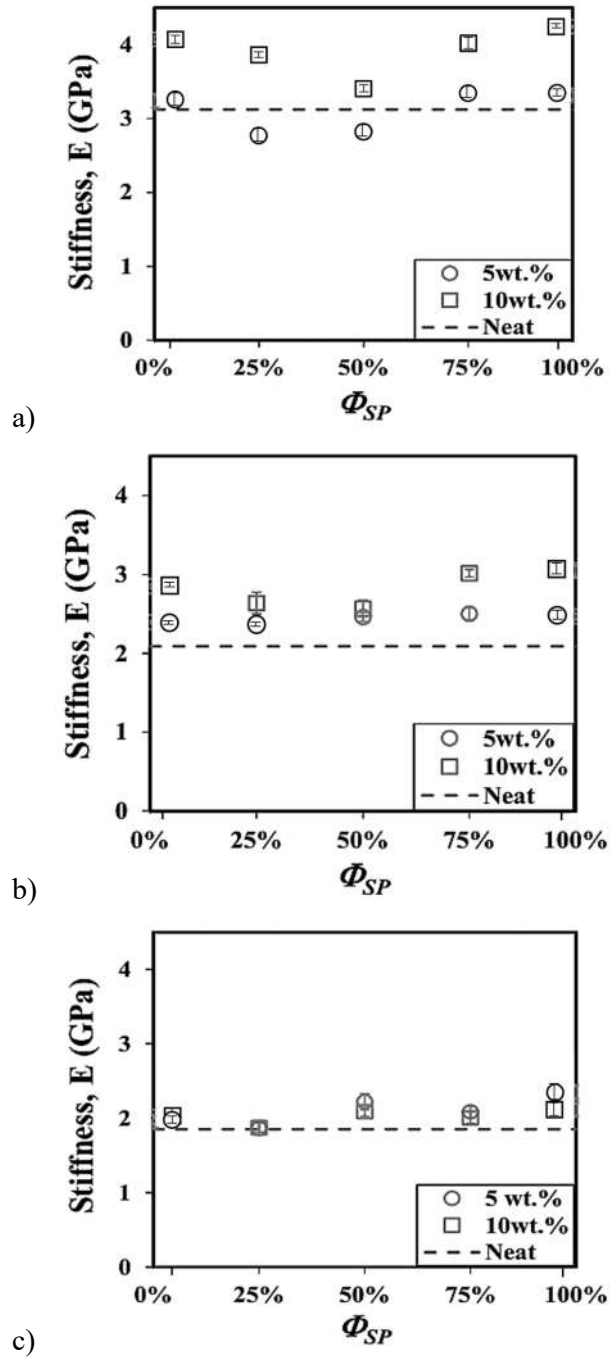


**Fig. 2-12** The dynamic stiffness nonmonotonic dependency on the particle composition ratio and weight fraction at (a)  $T=15^{\circ}\text{C}$ , (b)  $T=40^{\circ}\text{C}$ , and (c)  $T=50^{\circ}\text{C}$

In the present work it was observed that the stiffening effect due to increasing silica weight fraction was more obvious at room temperature (Fig. 2-12.a). However, indicated by small difference on the dynamic stiffness enhancement between 5% and 10% weight fractions, the stiffening effect was decreased with temperature increase (Fig. 2-12.b). Moreover, the influence of silica weight fraction on the dynamic stiffness can be neglected as temperature approached to  $T_g$  (Fig. 2-12.c). Such stiffness change indicated that, as temperature approached to  $T_g$ , the epoxy matrix became softer and more dominantly governed the dynamic stiffness behavior of the epoxy/silica composite. Similar stiffness change at high strain rate due to temperature increase had also been obtained by Gomez et al. [20], in the case of neat epoxy, and Owens et al. [73], in the case of epoxy filled with single size of silica particles.

The stress transmissibility increased with silica weight fraction at room temperature (Fig. 2-13). The increase of silica weight fraction enlarged the epoxy/silica interphase area. Due to strong adhesion of epoxy/silica, larger interphase area facilitated higher load transfer and thus, increased the stress transmissibility. However, the stress transmissibility enhancement of the epoxy filled with two sizes of silica particles was negligible compared to that filled with single size of silica particles. It indicated that two sizes of silica particles reduced the load transfer enhancement resulted from the increase of silica weight fraction. It is believed that the reduced load transfer between silica particle and epoxy matrix was caused by micro silica particle debonding which will be explained in the following section.



Loss energy performance of the epoxy/silica composite, despite of high deviations, was found to be increased with the weight fraction regardless the composition ratio of silica particles (Fig. 2-14). Neat epoxy exhibited low energy absorption due to its brittle nature during high strain rate loading. Cracks grew easily and resulted in fracture to such neat epoxy [87]. However, the energy absorption was found to be increased as silica particles introduced to the neat epoxy [88]. Deflected cracks growth due to the presence of silica particles increased the energy absorption in the epoxy/silica composite. Therefore, introducing higher silica weight fraction increased the energy absorption of epoxy/silica composite.

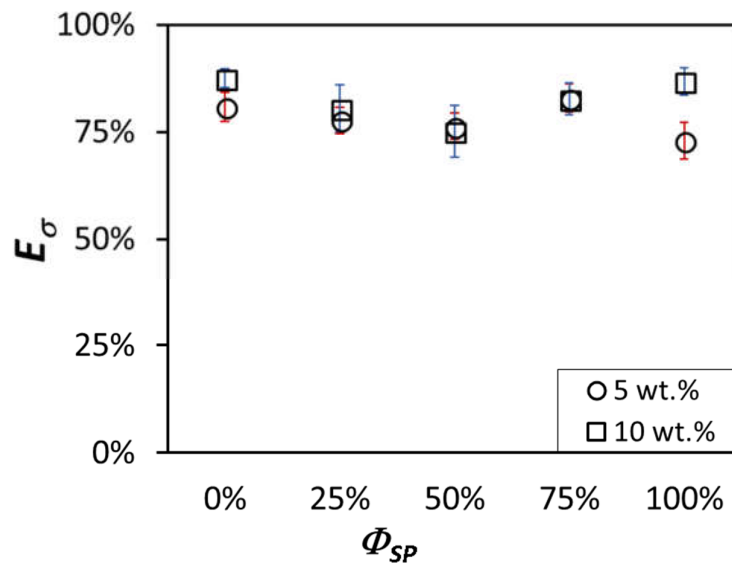


**Fig. 2-13** The nonmonotonic effect of particle composition ratio on the stress transmissibility at  $T = 15^\circ\text{C}$  according to Eq. (2-8.b).

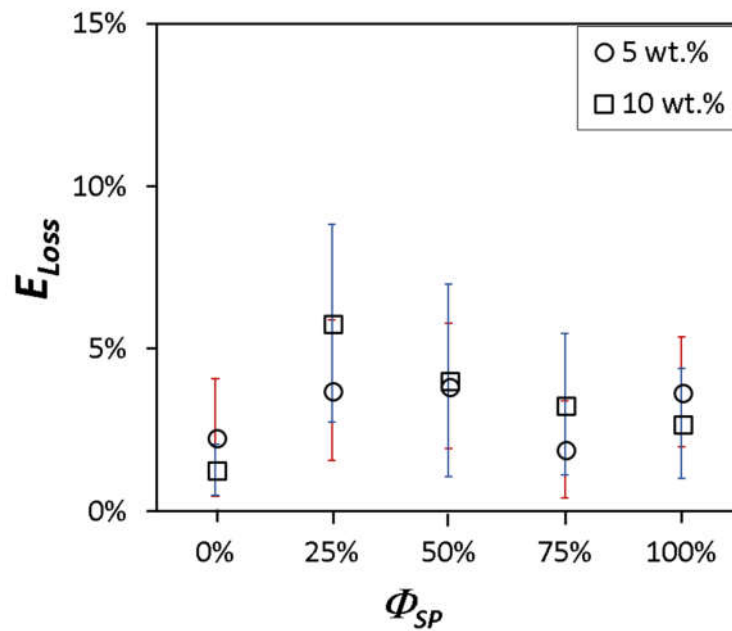


**Fig. 2-14** Nonmonotonic dependency of energy loss on the particle composition ratio at  $T = 15^\circ\text{C}$ .

#### 2.4.2 Effects of the composition ratio

Dittanet and Pearson [31] reported that the epoxy stiffness was slightly governed by the composition ratio of mixed micro and nano silica particles under static loading. It was reported that introducing nano silica weakened the bonding between micro silica and epoxy matrix. In the present work, a larger size ratio of micro and nano silica particle was used to modify the epoxy under high strain loading. Similar weakening effect on the dynamic stiffness and stress transmissibility was observed for the epoxy filled with two sizes of silica particles at room temperature (Figs. 2-12.a and 2-13). However, compared to the previous results of Dittanet and Pearson [31], a higher dependency of the epoxy dynamic stiffness and stress transmissibility on the silica composition ratio was found in the

present work. It was observed that the composition ratio of mixed micro and nano silica  $\Phi_{SP} = 50\%$  resulted in the minimum dynamic stiffness and stress transmissibility. Nevertheless, the influence of silica composition ratio on the dynamic stiffness became less significant as the temperature approached to  $T_g$  (Fig. 2-12.b for low weight fraction, and Fig. 2-12.c for all weight fractions).

In contrast with the dynamic stiffness, the loss energy performance of the epoxy filled with two sizes silica was higher compared to that filled with pure micro or nano silica particles. Loss energy performance also displayed significant dependency on the composition ratio of mixed micro and nano silica particles. It was observed that the loss energy was maximized at silica composition ratio  $\Phi_{SP} = 25\%$ . Interestingly,  $\Phi_{SP} = 25\%$  was found to be the optimum composition ratio which maximized the loss energy performance while provided high dynamic stiffness and stress transmissibility. The existence of the optimum composition ratio of micro and nano silica particles suggests that it is possible to modify the dynamic performance of the epoxy for appropriate practical applications.

In this chapter, the previous work of Dittanet and Pearson [31] and Wang et al. [26] are used to explain the sources of the weakening effects on the dynamic stiffness and the stress transmissibility. Using SEM (scanning electron microscope (SEM), Dittanet and Pearson [31] showed that silica microparticles debonded from the epoxy matrix. Such particles debonding were induced by the increase of stress concentration at the surface of microparticles owing to the presence of nanoparticles. Such particles debonding created voids which reduced the load

transfer between silica particles and epoxy matrix and thus, reduced the dynamic stiffness and stress transmissibility. Furthermore, Wang et al. [26] also reported that micro cracks were produced and propagated due to the stress concentration which is caused by the large size ratio of the two-size particles. In the present results, such particles debonding and cracks initiation are believed to occur during impacts and responsible for the decreases of the stiffness and stress transmissibility of the epoxy filled with silica micro-nanoparticles. Contrary, both voids created by debonding of micro silica particles and micro cracks facilitated more energy dissipation in the epoxy matrix. However, the epoxy matrix mobility was increased as the temperature approached to  $T_g$  and thus, minimized the influences of voids and cracks.

The deviations of the estimated stress transmissibility and loss energy performances were large (Figs. 2-13 and 2-14) due to the limitations of the experimental apparatus. The strain pulses used in the estimations were fluctuated during unloading period owing to the poor contact between specimen and the pressure bars. Despite such deviations, it is still worthy to analyze the tendencies of the averaged data.

## 2.5 Conclusions

The dynamic responses of epoxy adhesives were obtained using the SHPB tests. The effects of particle content and composition ratio of micro-nanoparticles on the dynamic responses of epoxy adhesive at the elevated temperature were

evaluated. At low temperature, the overall dynamic performances were governed by particle content and composition ratio. The dynamic stiffness, the stress transmissibility, and the energy loss were increased with the increase of particle content. Particle composition ratio exhibits nonmonotonic effects on the dynamic responses of epoxy/silica. The presence of micro-nanoparticles improved the energy loss at the expense of stiffness and stress transmissibility. At a temperature near  $T_g$ , however, the epoxy matrix governed the overall dynamic responses and thus, were less sensitive to the variations of particle content and composition ratio. The overall dynamic responses of epoxy adhesive were maximized by the presence of silica micro-nanoparticles at the optimum composition ratio of 25%.

## Chapter 3

# Synergistic effects of silica mixed micro and nanoparticles on the stiffness and damping of epoxy adhesives

### 3.1 Introduction

In lightweight structural applications such as spacecraft and automobile parts, epoxy-based adhesives and composites are superior to metal owing to their high strength-to-weight ratio and strong adhesion to different materials. Structures subjected to dynamic loads such as vibrations and impacts must be well-designed to ensure their safety, reliability, and comfort. Therefore, dynamic stiffness and damping characterizations of epoxy are critical for structural design and analysis.

In practice, high-modulus silica particles are commonly used to stiffen and toughen epoxy adhesive by exploiting inter-particle interactions, matrix–filler interactions, and the inherent properties of silica particles in a matrix. Well-dispersed silica nanoparticles stiffen and toughen an epoxy adhesive more efficiently than silica microparticles owing to their larger surface-to-volume ratio, forming a more substantial matrix–filler interphase area at a given weight fraction [27,32,42,76,89–91]. However, without any treatment, high-silica-content

nanoparticles are difficult to disperse uniformly using a conventional mechanical mixer and tend to aggregate/agglomerate in the epoxy matrix [34,36,37].

Composing an appropriate composition ratio between two sizes of silica particles for a given size ratio reduces viscosity and breaks up the agglomerate, thus improving particle dispersion [62,64,104,105]. Additionally, such bimodal silica particles induce more complex matrix–filler and inter-particle interactions, which generate concurring effects on epoxy dynamic properties [65,105,106]. Nevertheless, such deagglomeration effectivity over a wide range of silica weight fractions and its subsequent collaborative effects on epoxy dynamic stiffness and damping, especially at intermediate-strain-rate loading, have been given little attention.

Experimental work has been conducted to investigate the synergistic effects of two-size silica particles on epoxy stiffness and fracture energy absorption with respect to particle composition ratio. Kwon et al. [65,106] and Dittanet and Pearson [31] found an appropriate composition ratio of two-size silica particles that cooperatively toughens epoxy and ascribed this to better particle dispersion. Shariati et al. [66] found good dispersion at 1.5–6 wt.% for two-size silica nanoparticles of 17 and 65 nm diameters but did not find any considerable coactive effects on stiffness and fracture energy absorption. Such previous works have indicated that the interplay of particle content, size ratio, and composition ratio affect the particle distribution and subsequent collaborative effects, which is consistent with suggestions made by Greenwood et al. [62], [63] and Dames et al.

[64]. It is important to note that these previous studies focused on epoxy behavior under static loading, which may differ from that under dynamic loading owing to strain rate sensitivity of the epoxy and of matrix–filler interactions.

The effects of silica particles on epoxy behavior at high-strain-rate loading have been investigated using split Hopkinson pressure bars (SHPB). Miao et al. [48] and Tian et al. [72] reported that silica nanoparticles stiffen and strengthen epoxy composites at both quasi-static and dynamic loading. Silica nanoparticles stiffen epoxy efficiently at low-strain-rate loading [72]. Islam et al. [42] showed that dynamic stiffness increases with silica particle content dispersed in the epoxy matrix. However, such studies focused on single-size silica-filled epoxy dynamic behavior at high-strain-rate loading.

In the previous chapter, the elastic–dynamic stiffness and damping of epoxy filled with silica micro-nanoparticles were estimated using SHPB with sandwiched specimens under a strain rate loading of  $140 \text{ s}^{-1}$ . The epoxy filled with two-size silica particles exhibited greater damping, but lower stiffness compared to that of single silica particles. However, the damping was not precisely quantified because of the limitation of the sandwiched SHPB.

In the present chapter, the objective is to investigate the synergistic effects of silica micro-nanoparticles of varied composition ratio and weight fraction on epoxy dynamic stiffness and damping in the elastic region. The SHPB method with bonded specimens is used to generate a complete loading–unloading elastic stress–



strain response for epoxy filled with silica micro-nanoparticles and to precisely estimate damping.

The experimental evidence suggest that the deagglomeration effectivity and collaborative effects of silica micro-nanoparticles are limited by silica particle content and vary with the composition ratio. Silica micro-nanoparticles offer a simple and low-cost solution to the nanoparticle dispersion problem in conventional mechanical mixers; moreover, they provide options for designing epoxy dynamic stiffness and damping to cater for specific applications by varying the composition ratio.

This chapter presents the SHPB method with bonded specimens, data validation, and dynamic stiffness and damping estimations. It also reports and discusses the effects of silica micro-nanoparticle weight fraction and composition ratio on epoxy dynamic stiffness and damping.

## 3.2 Experimental method

The split Hopkinson pressure bar (SHPB) method has been widely used to characterize dynamic responses of solid materials. Up to date, the SHPB technique has been modified to adapt to tests of the various types of materials and those of small strain deformation [15,16,23,95–107]. The dynamic stiffness is represented by Young's modulus, which is estimated from the initial stress–strain slope. Hysteretic damping, which represents the ability of a material to dissipate

mechanical energy, is estimated from the area covered by a complete loading–unloading (closed-loop) stress–strain curve.

In SHPB test with sandwiched specimens, precise damping estimation is difficult owing to incomplete stress–strain responses, which are ascribed to poor bar–specimen contact during unloading. In the present work, epoxy/silica adhesive was bonded to both input and output bars to maintain bar–specimen contact and to generate closed-loop stress–strain responses.

### *3.2.1 Materials and specimen preparation*

The specimens were made from two-parts epoxy brand Scotch-Weld 1838 (B/A) filled with silica micro-nanoparticles. The physical properties of epoxy and silica particles are given in Table 3-1. The weight fraction and composition ratio of dispersed silica particles were varied as shown in Table 3-2. The specimens were prepared according to the following procedure to ensure consistency: first, silica micro-nanoparticles at the desired ratio were mixed with epoxy base (B) and accelerator (A) using a planetary centrifugal mixer and were then degassed. Second, the pressure bars' bonded areas were heated and the epoxy specimen of thickness and diameter equal to 5 and 20 mm were bonded between them. Finally, the specimens were cured at room temperature for 1 h and were then heated to 65 °C for 3 h. The specimen was cooled to room temperature for 24 h before testing.

**Table 3-1** Physical properties of epoxy and silica particles

Physical parameter	Epoxy		
	Micro silica	Nano silica	adhesive
Weight density (g/cm <sup>3</sup> )		2.65	1.21
Average diameter	34 $\mu$ m	17 nm	-
Specific surface area (m <sup>2</sup> /g)	3.4	80	-

**Table 3-2** Calculated surface area of pre-mixed silica micro-nanoparticles. Bracketed values indicate the conversion of silica content from weight fraction to volume fraction (calculated).

Composition ratio, $\Phi_{SP}$	Micro silica	Nano silica	Pre-mixed surface area (m <sup>2</sup> )		
			2 wt.%	5 wt.%	10 wt.%
			(1.01 vol.%)	(2.55 vol.%)	(5.24 vol.%)
0%	100%	0%	0.27	0.68	1.36
25%	75%	25%	1.80	4.51	9.02
50%	50%	50%	3.34	8.34	16.68
75%	25%	75%	4.87	12.17	24.34
100%	0%	100%	6.4	16	32

### 3.2.2 SHPB test apparatus

The SHPB used in the present work was composed of a striker bar, two pressure bars, and strain wave measurement instrumentation as shown in Fig. 3-1. All bars were made from carbon tool steel SK-5 with Young's modulus of 206 GPa and diameters of 20 mm. The impact side of the striker bar was slightly rounded to extend the rise time and avoid fluctuation in the early portion of the generated

incident pulse. The appropriate length of the pulse rise time ensures dynamic stress equilibrium in the specimen while a smooth incident pulse avoids distortion in the early part of the stress–strain response. Both characteristics are critical in obtaining valid and accurate data in SHPB tests.

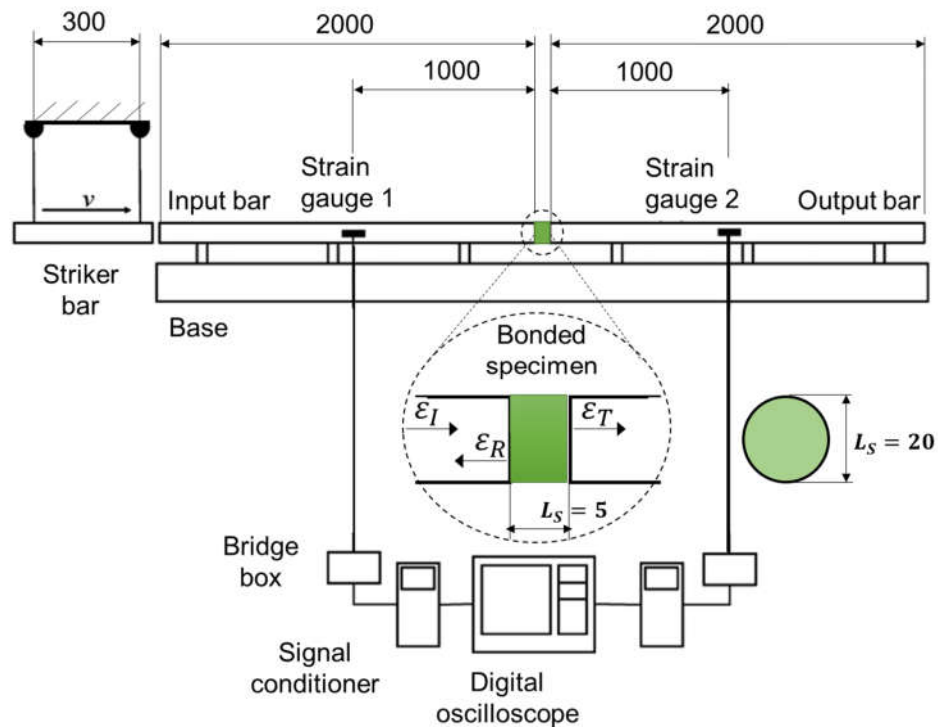


**Fig. 3-1** The SHPB apparatus with the bonded specimen (all dimensions are in mm)

A compressive incident pulse ( $\epsilon_I$ ) of 200  $\mu\text{s}$  in loading duration was generated during the impact of the striker bar on the input bar. At the bar–specimen interface, some part of the incident pulse is reflected ( $\epsilon_R$ ) to the input bar and the rest is transmitted ( $\epsilon_T$ ) to the output bar. Strain gauges were positioned in the middle of both pressure bars to avoid signal overlapping so that complete strain loading

and unloading could be recorded (Fig. 3-2). Such complete strain history for the specimen resulted in a completely closed-loop stress–strain response, which is required to accurately estimate damping.

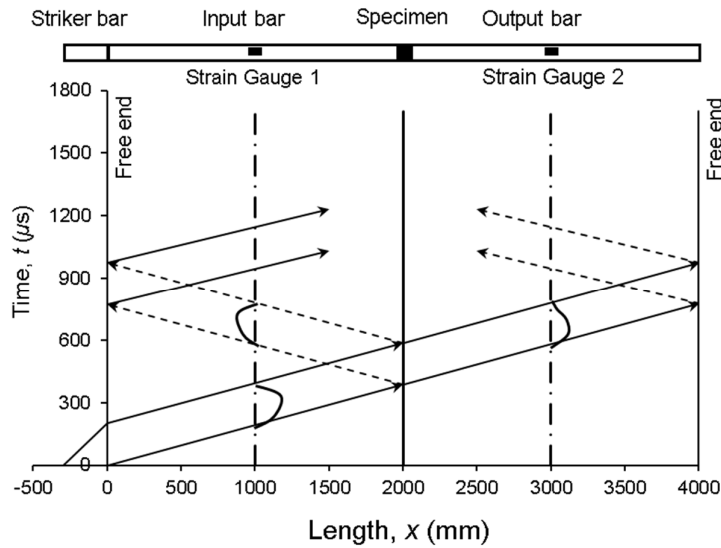


**Fig. 3-2** Split Hopkinson bar arrangement and Lagrangian diagram showing gauge locations that avoid overlap of the measured strain waves.

### 3.2.3 Calibration and data validity

A calibration test was conducted on pressure bars without specimens to ensure the validity and accuracy of the obtained data. Identical incident and transmitted pulses obtained from measurement of pressure bars without specimens (Fig. 3-3) indicated good alignment of the SHPB system and ensured that the reflected pulse measured in Fig. 3-4 was contributed only by the specimen.

Fig. 3-4 shows that the crowned striker bar effectively generated a smooth incident pulse with appropriate rise time. This ensured that the dynamic equilibrium

condition in the specimen during loading and unloading was achieved, as shown in Fig. 3-5. The forces at both sides of the specimens are formulated as:

$$P_1 = A_B E_B \{\varepsilon_I(t) + \varepsilon_R(t)\} \quad (3 - 1)$$

$$P_2 = A_B E_B \varepsilon_T(t) \quad (3 - 2)$$

where  $A_B$  is the pressure bars' cross-sectional area,  $E_B$  is Young's modulus of the bars, and  $\varepsilon_I$ ,  $\varepsilon_R$ , and  $\varepsilon_T$  are the aligned incident, reflected, and transmitted pulses, respectively.

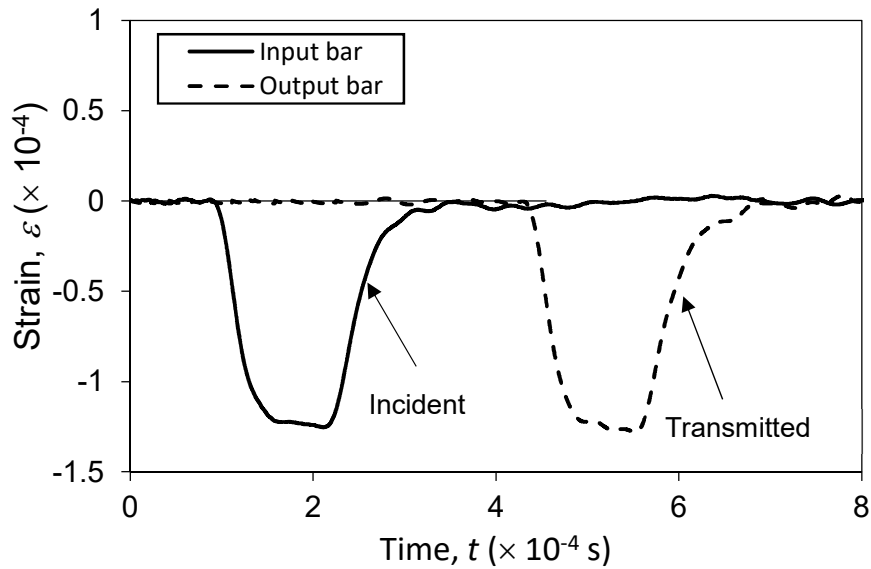


**Fig. 3-3** Recorded signals of bar alignment. Nearly identical pulses of the incident and transmitted, and the absence of reflected pulse confirmed that the bar system is in good alignment.

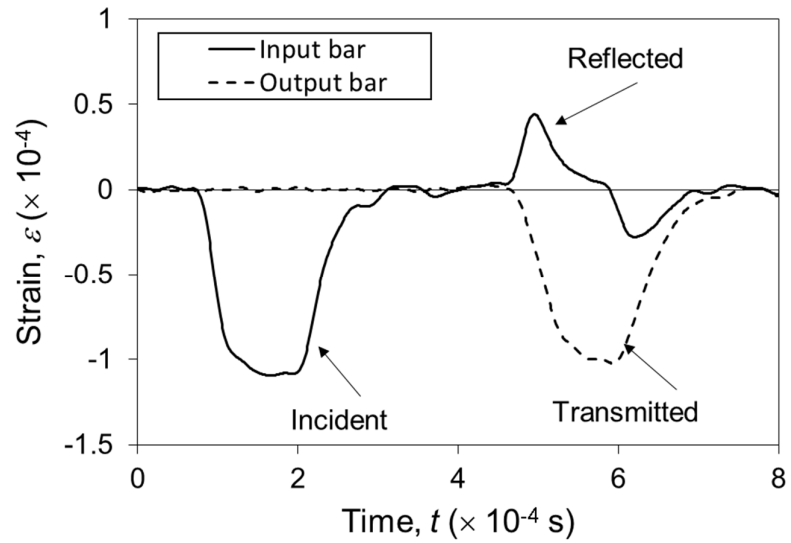


**Fig. 3-4** Recorded stress wave from a typical measurement with a specimen

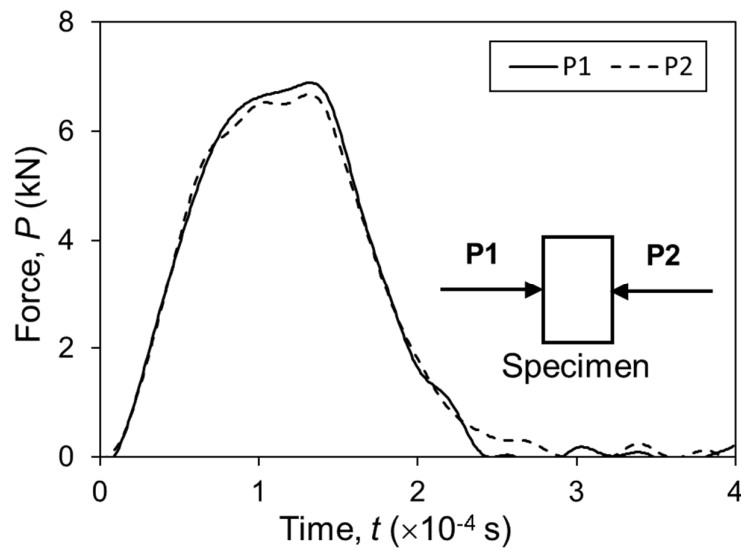


**Fig. 3-5** Dynamic stress equilibrium on both sides of the specimen.

The nearly constant strain rate during the test period was not obtained, as represented by the reflected wave in Fig. 3-4, owing to the limitation of the pulse-shaping technique used and the bonded constraints at the interface of specimen and pressure bars. However, such strain acceleration does not significantly affect the estimations and analysis of dynamic stiffness and damping in the present measurement condition.

### 3.2.4 Estimation of stiffness and damping

Validated SHPB data were used to generate stress–strain responses (Fig. 3-6) for the specimens using the following equations:

$$\sigma_n = \frac{A_B}{A_S} E_B \varepsilon_T(t) \quad (3 - 3)$$

$$\dot{\varepsilon}_n = \frac{2C_0}{L_S} 2\varepsilon_R(t) \quad (3 - 4)$$

$$\varepsilon_n = \frac{2C_0}{L_S} \int \varepsilon_R(t) dt \quad (3 - 5)$$

where  $\sigma_n$  is the stress,  $\varepsilon_n$  is the strain,  $C_0$  is the elastic wave speed through the bars,  $L_S$  and  $A_S$  are the thickness and the surface area of the specimen, respectively, and  $t$  is the time duration.

The stress–strain in the small strain range was nearly linear. Dynamic stiffness was estimated by fitting the slope of the line to the initial part of the stress–strain curve in Fig. 3-6. Hysteretic damping was estimated from the integral of the closed-loop area of the stress–strain curve using the following equation:

$$\delta = \int \sigma_n(t) d\varepsilon_n(t) \quad (3 - 6)$$



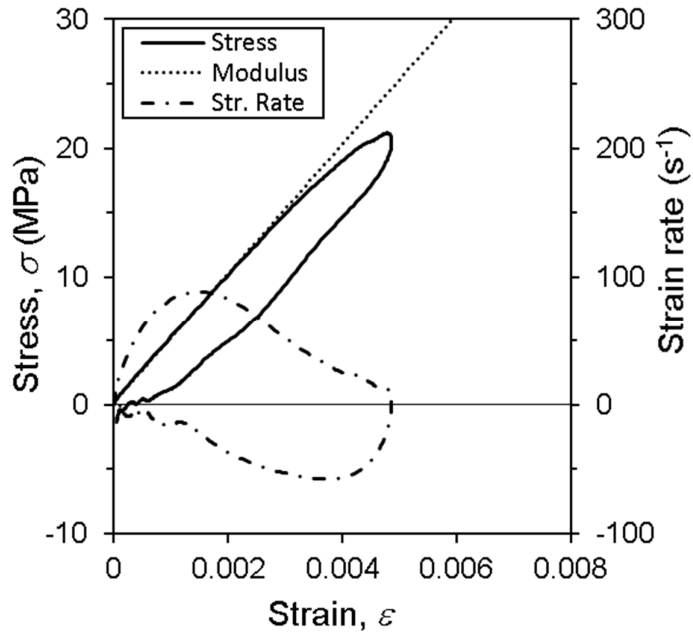


**Fig. 3-6** Estimation of stiffness and damping from the slope and closed-loop area of the stress-strain response. In the analysis, the strain rate is averaged from the loading part.

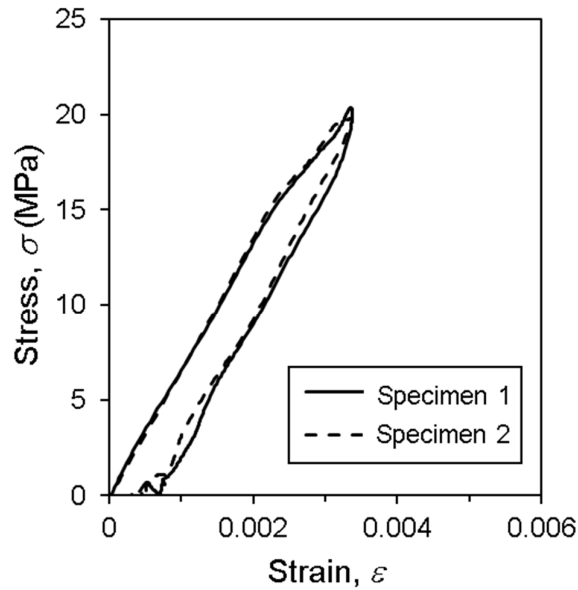


**Fig. 3-7** Overlapped stress-strain responses of two epoxy/silica specimens indicate the reproducibility and consistency of experiments.

The reproducibility and consistency of measured data are indicated by the nearly overlapped stress–strain response of two specimens with a given silica weight fraction and composition ratio, as shown in Fig. 3-7.

### 3.3 Results and discussions

Tests were conducted to investigate the effects of silica micro-nanoparticles on the dynamic compressive stiffness and damping of epoxy adhesive. A set of SHPBs with bonded specimens was used to generate stress–strain loops at the average strain rate of  $80 \pm 10 \text{ s}^{-1}$ . Several tests were conducted on each specimen, and the average value obtained was used in the analyses.

Stiffness and damping were estimated from the initial slope (modulus) and loop area of stress–strain responses, respectively. The effects of silica particles on the stiffness and damping of epoxy/silica adhesive were investigated for evaluation. Figures 3-8 and 3-9 show the stiffness and damping behaviors of epoxy/silica adhesive at silica contents of 2, 5, and 10-wt.%, as the silica composition ratio varies from pure microparticles ( $\Phi_{SP}=0\%$ ) to pure nanoparticles ( $\Phi_{SP}=100\%$ ).

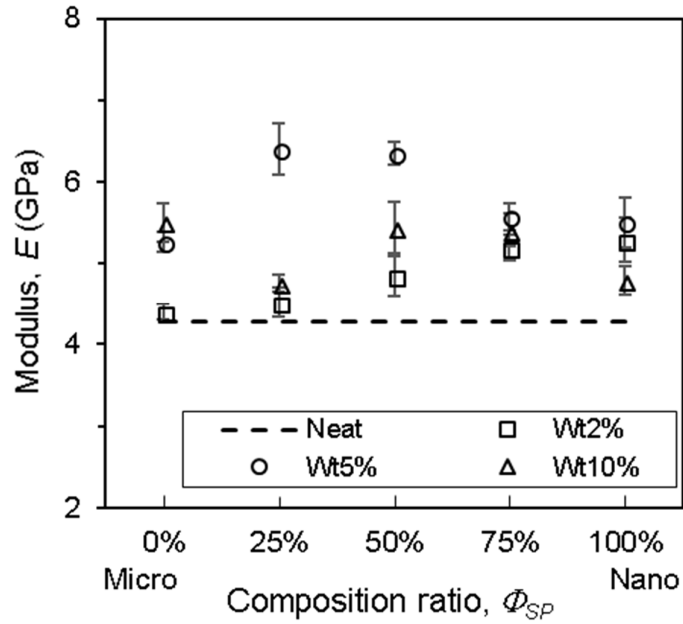


Fig. 3-8 Effects of silica content and composition ratio on the dynamic stiffness of epoxy.

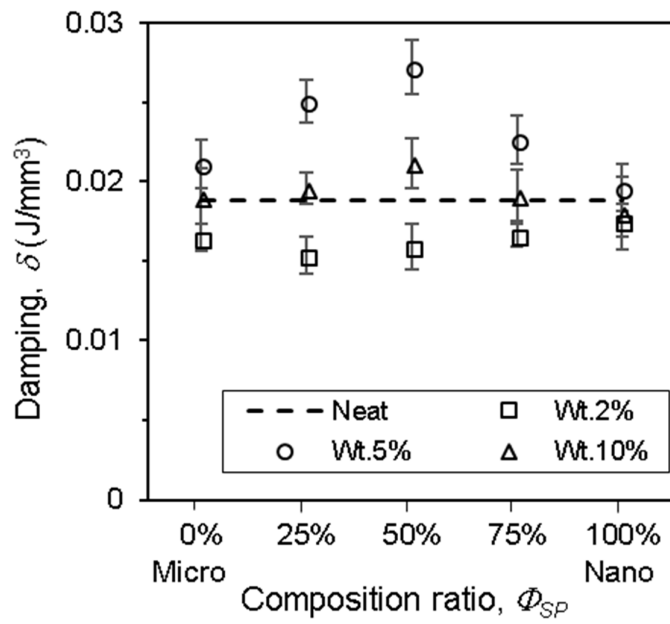


Fig. 3-9 Effects of silica content and composition ratio on the hysteretic damping of epoxy.

The epoxy stiffness increased monotonically with increasing nanoparticle portion at a silica content of 2-wt.% (Fig. 3-8). The influence became nonmonotonic with the increase of silica content to values of 5 and 10-wt.%. The stiffness of epoxy silica for any composition ratio increased with the increase of silica content up to 5-wt.%. However, the epoxy stiffness dropped as the silica particle content increased to 10-wt. %. At a silica content of 5-wt.%, it was observed that the stiffening effect of two-size silica was superior than that of single-size silica. The greatest stiffening effect of two-size silica at 5-wt.% was observed at the composition ratio of 25%, where epoxy stiffness increased by 45% compared to that of neat epoxy.

The epoxy damping was nonmonotonically reduced by up to 14% with the two-size particles at a low silica content of 2-wt.% (Fig. 3-9). Significant increases in epoxy damping occurred with the presence of two-size silica particles of any composition ratio as silica content increased to 5-wt.%. The highest epoxy damping was obtained at silica content of 5-wt.% and a composition ratio of 50%, where damping increased by 40% compared to that of neat epoxy. The damping reduced as silica content increased further to 10-wt.%.

Deviations were observed for both the estimated stiffness and damping. The main sources of deviations were variations in the specimens due to the mixing process. Initial slope fitting in stiffness estimation and fluctuating stress–strain loops near the end of the unloading stage also contributed to stiffness and damping

deviations, respectively. Four specimens were used for each test condition to minimize deviation.

### 3.3.1 Effects of silica micro-nanoparticles on dynamic stiffness

It has been reported that dispersed silica particles form a matrix–filler interphase area stiffer than the matrix and therefore stiffen and restrict deformation of epoxy adhesives [26,50]. Epoxy stiffness increases with the interphase area formed in the matrix, which is affected by the surface area of silica particles and particle dispersion quality.

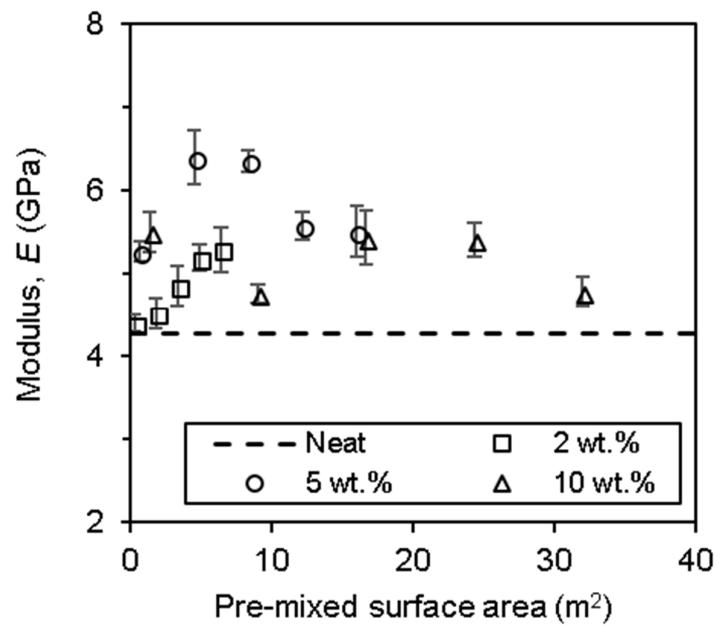
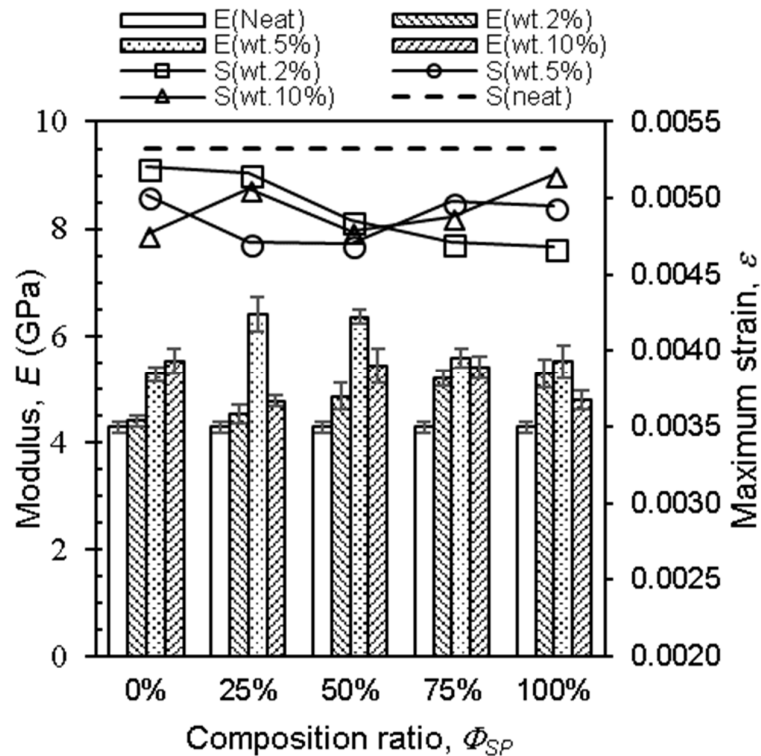


Fig. 3-10 Effects of silica content and pre-mixed surface area on the epoxy stiffness

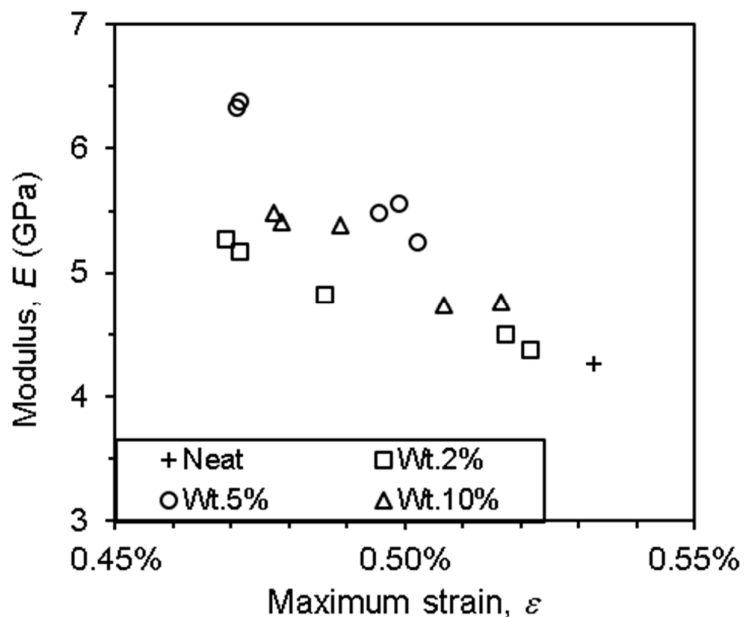
Fig. 3-8 shows the stiffening effect of silica micro-nanoparticles at different weight fractions and composition ratios. A collaborative stiffening effect is only found on the epoxy filled with 5-wt.% silica micro-nanoparticles. At 5-wt.% silica content, micro-nanoparticles generate a stronger stiffening effect on the epoxy compared to those of either pure microparticles or pure nanoparticles. Fig. 3-8 also reveals that 10-wt.% silica particles generate less stiffening effects on epoxy adhesives even though it has a larger surface area owing to the higher particle content. This result shows the critical role of particle dispersion in the formation of effective interphase area that stiffen epoxy adhesive. As a conventional mechanical mixer was used in the present work in the absence of any chemical treatment, dispersion quality was affected by particle size and weight fraction.

Figure 3-10 highlights the effects of silica weight fraction and composition ratio on the transformation of particles surface area into effective interphase area that stiffens an epoxy adhesive. The surface area was computed from the specific surface area of silica particles (Table 3-1) at given composition ratios and weight fractions. At a given weight fraction, the surface area increased sequentially with the increase of nanoparticles portion from pure microparticles ( $\Phi_{SP} = 0\%$ ) to pure nanoparticles ( $\Phi_{SP} = 100\%$ ) along the horizontal axis of Fig. 3-10. Large surface area of 10-wt% silica particles produced lower stiffening effect compared to that of 5-wt.% silica particles which has smaller surface area. Thus, 5-wt.% silica micro-nanoparticles formed larger interphase area compared to that 10-wt.% silica. Particularly, 5 wt.% silica with a nanoparticle proportion of less than 75% effectively form large effective interphase areas, thereby generating a strong

stiffening effect. In the case of 2 wt.% silica, micro-nanoparticles have only a weak effect on the formation of an effective interphase area. Pure nanoparticles at 2 wt.% silica are well dispersed, achieving a large effective interphase area; therefore, these provide stronger stiffening effects than those of micro-nanoparticles. Good dispersion of low-content silica nanoparticles was observed, which is in agreement with previous works by Bondioli et al. [34], Zheng et al. [36], and Feli and Jalilian [37]. This result suggests that composing silica micro and nanoparticles in appropriate ratios improves their dispersion up to certain weight fraction even when using only a conventional mechanical mixer.



**Fig. 3-11** (a) The simultaneous effects of silica on the stiffness and strain reducing,  $E$  for stiffness and  $S$  for the strain.



**Fig. 3-11 (b)** Proportional stiffness–strain relation representing the effective interphase area formed in the matrix.

The effectiveness of silica micro-nanoparticles in improving silica nanoparticle dispersion was verified by comparing the stiffness and strain response of the epoxy adhesive. Figs. 3-11.(a) and (b) shows the epoxy stiffness and strain responses of the epoxy adhesive used to estimate and compare the effective interphase area. As previously mentioned, the interphase area simultaneously increases the stiffness and restricts the strain deformation of epoxy. Thus, the epoxy with higher stiffness and smaller strain deformation contained a larger interphase area. Consequently, neat epoxy exhibited the lowest stiffness and largest strain deformation because it contained no interphase area as shown in Fig. 3-11.(a) and



the lower-right quadrant of Fig. 3-11.(b). Epoxy filled with 5 wt.% silica micro-nanoparticles and composition ratio 25% and 50% exhibited the largest interphase area which is indicated by high stiffness and small strain as seen in Fig. 3-11.(a) and the upper-left quadrant of Fig. 3-11.(b). Epoxy filled with 5 wt.% silica micro-nanoparticles was the most sensitive to composition ratio variations; this was indicated by stronger stiffness–strain response with steeper slopes as shown in Fig. 3-11.(b). The epoxy filled with 10 wt.% silica micro-nanoparticles exhibited a smaller interphase area and was less sensitive to composition ratio compared to the case of 5 wt.%. This result confirms that composing silica micro and nanoparticles effectively improves nanoparticle dispersion for silica content up to 5 wt.% and generates a synergistic stiffening effect. It is worth noting that silica nanoparticle:microparticle compositions of 25%:75% or 50%:50% increase epoxy stiffness by 45% compared to that of neat epoxy.

In previous studies, Kwon et al. [65], [93], Dittanet and Pearson [31], and Shariati et al. [66], did not obtain a considerable cooperative stiffening effect of well-dispersed two-size silica particles. Kwon et al. and Shariati et al. mixed two-size silica particles, which have smaller size ratios ( $1.56\ \mu\text{m}:0.24\ \mu\text{m}$  and  $17\ \text{nm}:65\ \text{nm}$  in diameter, respectively) than that used in the present work ( $34\ \mu\text{m}:17\ \text{nm}$ ). Such smaller size ratios might be less effective in improving the interphase area and generating collaborative stiffening effects. Olhero and Ferreira found that a larger size ratio of mixed silica particles resulted in better deagglomeration and thus better dispersion [108].

Dittanet and Pearson [31], however, combined silica particles of 42  $\mu\text{m}$  with 23, 74, and 170 nm, but did not observe any considerable synergistic stiffening effect. It was reported by Dittanet and Pearson in the same paper that the stiffening effect of the interphase area was negligibly small owing to weak matrix–filler adhesion.

Notably, Fig. 3-11.(b) shows comparable ranges of strain deformations of epoxy filled with any silica weight fraction despite their different interphase areas. Higher interphase area should restrict deformation of the epoxy adhesive. This fact may indicate the existence of additional deformations induced by matrix–filler interactions. Particle debonding and stress concentration induce local matrix yielding or plastic deformation around the interphase area. The mechanism of such deformations and its contribution to energy dissipation is discussed in the next section.

An alternative explanation for the additional strain deformation is a softer epoxy matrix due to poor cross-linking between the epoxy base and its hardener. Olhero and Ferreira reported that high nanoparticle content increases viscosity, and hence it is difficult to obtain homogeneous mixing [108]. Tarrío-Saavedra showed that higher nanoparticle content forms agglomerates that prevent perfect mixing of some part of the epoxy base and its hardener [109].

The results of this paper suggest that the poor dispersion performance of a conventional mechanical mixer can be improved by composing appropriate ratios of silica micro-nanoparticles. A synergistic stiffening effect is generated by the

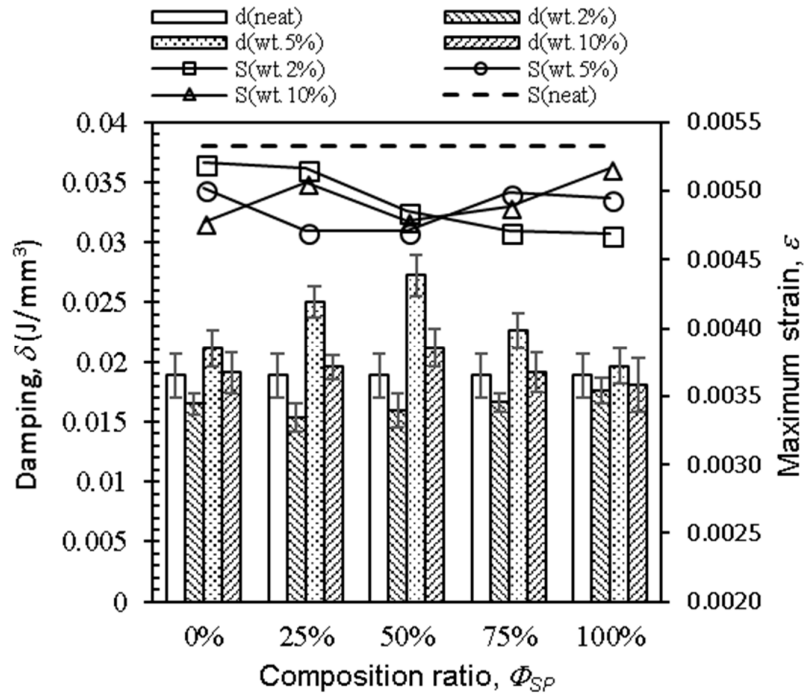
improved dispersion of silica nanoparticles up to a silica content of 5 wt.%. Beyond that silica content, mixed micro-nanoparticles with diameters of 34  $\mu\text{m}$  and 17 nm are less effective in improving dispersion. However, using two-size particles, which have different size ratios, may generate different results.

### 3.3.2 *The synergistic effect of silica micro-nanoparticles on hysteretic damping*

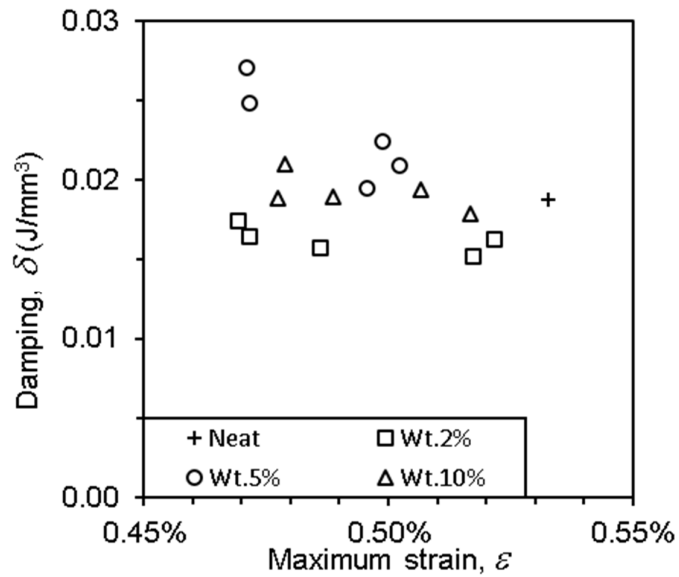
Owing to its inherent viscoelasticity, neat epoxy dissipates energy through internal friction during deformation, which can be estimated from the stress-strain loop area curve, as shown in Fig. 3-6.

The presence of high-modulus silica particles reduces epoxy deformation and thus reduces energy dissipation in the epoxy matrix. Therefore, the energy dissipation of epoxy with a silica content of 2 wt.% is lower than that of neat epoxy, as shown in Fig. 3-12. Epoxy damping is reduced by 14% by the presence of 2 wt.% silica particles. Inter-particle slipping and friction in the nanoparticle aggregates might facilitate energy dissipation as demonstrated by Yang et al. [110].

The energy dissipation values for epoxy with silica contents of 5 and 10-wt.%, however, are larger than that for neat epoxy. This increased energy dissipation indicates the existence of other energy dissipation mechanisms induced by matrix-filler interactions.



(a)



(b)

**Fig. 3-12** (a) The simultaneous effects of silica on the damping and strain reducing, d for damping and S for the strain. (b) Damping-strain relation of epoxy/silica and neat epoxy.

There are several mechanisms of energy dissipation induced by matrix–filler interactions suggested in previous works [31], [67], [111]. Crack pinning and crack bridging are dominant energy dissipation mechanisms for epoxy filled with pure silica microparticles. In epoxy filled only with nanoparticles, energy is dissipated by local plastic deformation and matrix shear yielding induced by the nanoparticles debonding.

Epoxy filled with two-size silica particles exhibits superior energy dissipation to that of single-size silica particles owing to more complex matrix–filler interactions [31], [67]. This arises because of synergetic mechanisms which boost epoxy energy dissipation such as nanoparticles and microparticles debonding followed by subsequent void formation and growth, crack deflection, and branching. In the present work, damping increases by 40% compared to that of neat epoxy at a silica content of 5 wt.% composed of 50% microparticles and 50% nanoparticles.

The mechanisms mentioned above result in additional strain deformation in epoxy with 5 and 10 wt.% silica, as confirmed in the previous subsection. There is evidence of yielding or damage occurrence: stress–strain responses deviate [112], [113] from linear slopes, as shown in Fig. 3-13.

There is also evidence of a disturbance in the specimen stress equilibrium during unloading, which may indicate damage in the epoxy/silica, as shown in Fig. 3-14. However, it is not clear whether this disturbance is caused by crack opening or by void expansion due to tension in the specimen. Damage also contributes to

energy dissipation via cracks in the matrix and matrix/particle slipping in the interphase area [110], [114].

Epoxy damping decreases as the silica content increases to 10 wt.%. The reduced matrix volume is one factor responsible for this lower damping performance. However, considering the small matrix volume reduction by the addition of 10 wt.% silica particles (equal to 5.24 vol.%, Table 3-2), it is inappropriate to ascribe poor damping performance to this matrix volume reduction alone.

As mentioned in the previous section, poor cross-linking between the epoxy base and its hardener is likely to occur. Some parts of the matrix that are poorly crosslinked do not exhibit viscoelastic properties such as hysteretic damping. Thus, the effective matrix volume, which enables energy dissipation, is reduced and results in poor damping performance.

The results in this study suggest that the damping performance of epoxy/silica is influenced by both inherent matrix properties and by matrix–filler interactions. Damping can be increased by adequate dispersal of an appropriate amount of two-size silica particles in an epoxy matrix, which generate cooperative matrix–filler interactions to dissipate energy.

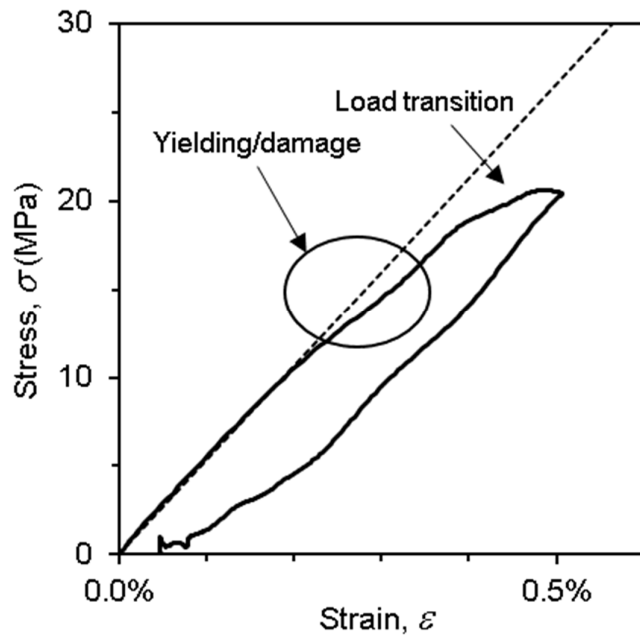


**Fig. 3-13** Yield-like or damage behavior indicated by deviation of the stress-strain response from its straight elastic line.

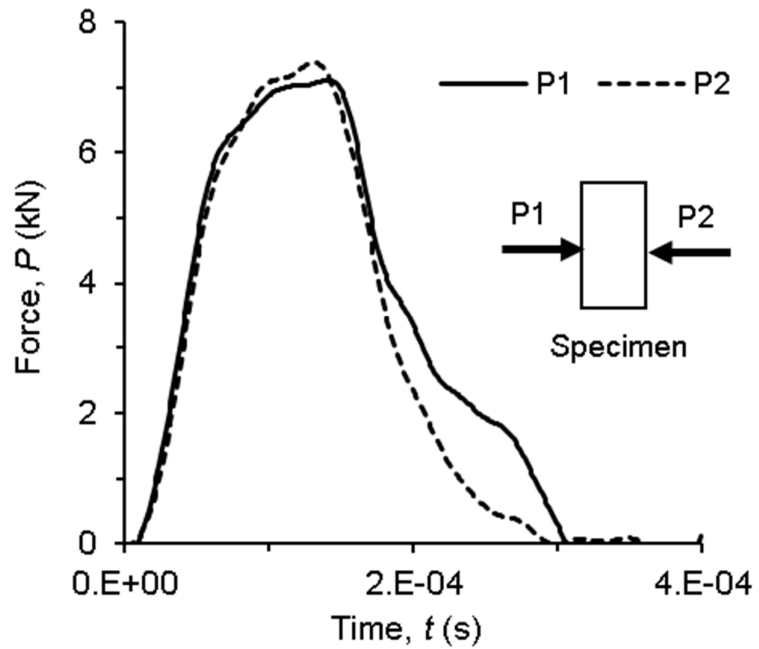


**Fig. 3-14** Damage indication, which disturbed the stress equilibrium during unloading.

3.3.3 Optimum composition ratio and weight fraction of silica micro-nanoparticles

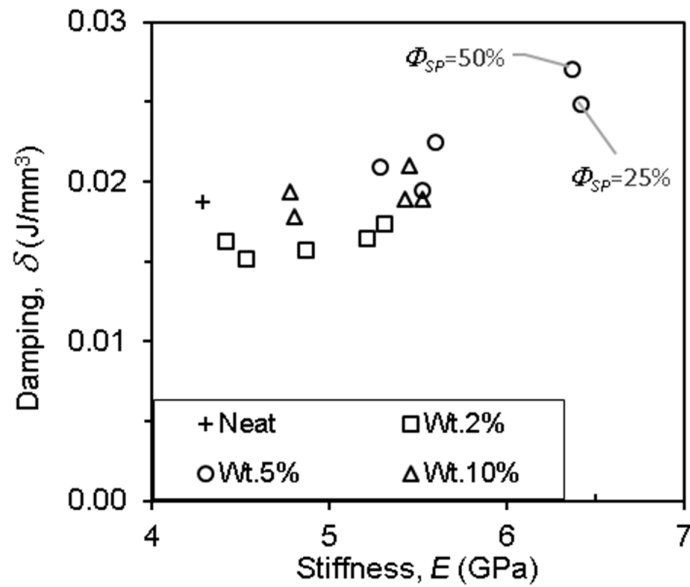


**Fig. 3-15** Synergistic effects of mixed silica micro-nanoparticles on stiffness and damping performance.

Fig. 3-15 summarizes the influences of silica micro-nanoparticles on dynamic stiffness and hysteretic damping of epoxy adhesives. There was no synergy effect at a low silica content of 2 wt.% owing to the dominant effect of nanoparticles. Using pure silica nanoparticles was more beneficial than using micro-nanoparticles in that doing so efficiently stiffened the epoxy adhesive without reducing damping excessively.

A silica content of 5 wt.% provided a wide range of stiffness and damping performance when varying the composition ratio; therefore, it furnishes a wide array of options for designing dynamic properties of epoxy adhesives appropriately



for their applications. Moreover, both stiffness and damping can be increased by 45% and 40%, respectively, at the optimum composition ratio of  $\Phi_{SP} = 50\%$ .

In contrast, a silica content of 10 wt.% was less sensitive to the composition ratio and provided only weak performance in terms of stiffness and damping, which is a disadvantage in design applications. The best synergy effect at this silica content was obtained for higher microparticle proportions relative to nanoparticle proportions ( $\Phi_{SP} = 25\%$ ).

### 3.4 Conclusions

The synergistic effects of silica micro-nanoparticles on the dynamic stiffness and damping of a bonded epoxy adhesive were investigated using split Hopkinson pressure bars. The effectiveness of selecting ratios of silica micro and nanoparticles for improving silica particle dispersion was discussed.

In the range of measurement, silica micro-nanoparticles of 34  $\mu\text{m}$  and 17 nm in average diameter, respectively, effectively improved nanoparticle dispersion, providing increased matrix–filler interaction through larger interphase areas. Therefore, this composition generated synergistic stiffening and energy absorption effects in epoxy with a silica content of 5 wt.%. The synergistic stiffening effect was generated by the increased interphase area due to the improved dispersion of the silica nanoparticles. The synergistic energy absorption effect was generated by yield and damage induced by complex interactions between the epoxy matrix and the silica micro-nanoparticles.

The effectiveness of silica micro-nanoparticles for improving the dispersion of silica particles is limited to 5 wt.% when using a conventional mechanical mixer like the one used in this paper. However, there are possibilities for improving deagglomeration quality at higher silica contents using an appropriate composition ratio of two-size silica particles with a larger particle size ratio.

The present paper provides experimental observations of epoxy dynamic stiffness and damping characteristics influenced by mixed silica micro-nanoparticles. By obtaining these characteristics, epoxy dynamic performance can be engineered for appropriate structural applications wherein epoxy is subjected to impact and vibration, such as in automobiles. In future work, another energy dissipation mechanism that avoids damage should be considered using hybrid filler materials such as a combination of soft and hard fillers.

Although yield or damage behavior, which contributes to energy dissipation, was identified and explained in this paper, a thorough investigation of matrix–filler interactions remain for future work to develop a better understanding of dynamic damping mechanisms.

## Chapter 4 Conclusions

### 4.1 The conclusions of the present studies

In the present study, the split Hopkinson pressure bar tests have been carried out to generate stress-strain responses of the epoxy adhesive under impact loads. The stiffness and damping of the epoxy adhesive have been estimated from the slope and the loop area of the stress-strain responses, respectively. The influences of silica weight fraction and composition ratio of the micro-nanoparticles on the stiffness and damping of the epoxy adhesive have been evaluated. The silica weight fractions given are 2, 5, and 10-wt.% and the composition ratio was varied from pure micro to pure nanoparticles. The evaluation of dynamic performances has been conducted at the increased temperature of 15°C, 40°C, and 50°C. Furthermore, the results have been evaluated for the synergetic effects of silica micro-nanoparticles and the mixture rule which improves both stiffness and damping.

Silica micro and nanoparticles synergistically provide higher stiffening effects and facilitate higher energy absorptions compared to pure micro or nanoparticles. Such synergetic effects are generated from the improved particle dispersion which increases the intensity of the interactions between the epoxy matrix and silica micro-nanoparticles. The superior stiffness of epoxy with two-size particles is facilitated by the formation of larger interphase; while the higher damping is facilitated by the damages and local plastic deformations induced by the

synergetic interactions between micro-nanoparticles and the matrix. The optimum composition ratio of 50% at silica weight fraction of 10% maximizes both the stiffness and the damping of epoxy adhesive by 45% and 40%, respectively. The reinforcing effects of silica micro-nanoparticles are still significant at high temperature ( $T=40^{\circ}\text{C}$ ).

The present study has demonstrated the effectiveness of silica micro-nanoparticles to modify the stiffness and damping of epoxy adhesive. The mixture rule provides a wide range of design options to modify the dynamic performances of epoxy adhesive to match the applications. The key result of the present study is the simultaneous improvements on both the stiffness and damping provided by mixed silica micro-nanoparticles. Both stiffness and damping are crucial to maintain the structural rigidity and reliability, as well as to reduce the noise and vibration. Furthermore, the results of this study suggest a simple and low-cost alternative technique to exploit the reinforcing effects of silica nanoparticles without any additional mixing process.

However, the effectiveness of silica micro-nanoparticles to improve particles dispersion and produces such synergistic effects is limited by the viscosity of the epoxy matrix, the weight fraction of silica particles, and the mixing process. In the present study, pre-heating the epoxy matrix and applying sequential mixing of epoxy with silica micro-nanoparticles improve particle dispersion up to 5-wt.% even with a conventional planetary-centrifugal mixer. However, this technique is

less effective to improve particles dispersion at higher silica weight fraction of 10% due to the increase of viscosity with the presence of higher silica content.

## 4.2 The outlook for future research

Regarding the beneficial effect of two-size particles for improving the epoxy adhesive performance and the limitations in the present study, it is interesting to conduct future works on:

1. The effects of silica micro-nanoparticles on the structural joint performances under impact loadings, including tensile loadings.
2. Combining silica micro-nanoparticles with particles of high inherent damping, such as Pb-Sn hollow-tubes and carbon nanotubes, which improve the damping by deforming themselves instead of inducing matrix damages.
3. Developing the SHPB apparatus to deal with a test at small strain loading which is required to characterize elastic behaviors of adhesive materials and other materials with similar natures.

## Reference

- [1] I. Higuchi, T. Sawa, and H. Okuno, “Three-dimensional Finite Element Analysis of Stress Response in Adhesive Butt Joints Subjected to Impact Tensile Loads,” *Journal of Adhesion*, vol. 69, no. 1–2, pp. 59–82, Jan. 1999.
- [2] L. Liao and T. Sawa, “Finite element stress analysis and strength evaluation of epoxy-steel cylinders subjected to impact push-off loads,” *International Journal of Adhesion and Adhesives*, vol. 31, no. 5, pp. 322–330, Jul. 2011.
- [3] R. Hazimeh, G. Challita, K. Khalil, and R. Othman, “Finite element analysis of adhesively bonded composite joints subjected to impact loadings,” *International Journal of Adhesion and Adhesives*, vol. 56, pp. 24–31, Jan. 2015.
- [4] M. Asgharifar, F. Kong, B. Carlson, and R. Kovacevic, “Dynamic analysis of adhesively bonded joint under solid projectile impact,” *International Journal of Adhesion and Adhesives*, vol. 50, pp. 17–31, Apr. 2014.
- [5] Y. Fan, X. Gong, S. Xuan, L. Qin, and X. Li, “Effect of Cross-Link Density of the Matrix on the Damping Properties of Magnetorheological Elastomers,” *Industrial & Engineering Chemistry Research*, vol. 52, no. 2, pp. 771–778, Jan. 2013.

- [6] R. J. C. Carbas, E. A. S. Marques, L. F. M. da Silva, and A. M. Lopes, “Effect of Cure Temperature on the Glass Transition Temperature and Mechanical Properties of Epoxy Adhesives,” *The Journal of Adhesion*, vol. 90, no. 1, pp. 104–119, Jan. 2014.
- [7] R. J. C. Carbas, L. F. M. da Silva, E. A. S. Marques, and A. M. Lopes, “Effect of post-cure on the glass transition temperature and mechanical properties of epoxy adhesives,” *Journal of Adhesion Science and Technology*, vol. 27, no. 23, pp. 2542–2557, Dec. 2013.
- [8] F. Lapique and K. Redford, “Curing effects on viscosity and mechanical properties of a commercial epoxy resin adhesive,” *International journal of adhesion and adhesives*, vol. 22, no. 4, pp. 337–346, Jan. 2002.
- [9] X. Wang, H. Liu, and S. Ouyang, “Damping properties of flexible epoxy resin,” *Journal of Wuhan University of Technology-Material Science Edition*, vol. 23, no. 3, pp. 411–414, Jun. 2008.
- [10] A. Bandyopadhyay, P. K. Valavala, T. C. Clancy, K. E. Wise, and G. M. Odegard, “Molecular modeling of crosslinked epoxy polymers: The effect of crosslink density on thermomechanical properties,” *Polymer*, vol. 52, no. 11, pp. 2445–2452, May 2011.
- [11] A. Shokuhfar and B. Arab, “The effect of cross linking density on the mechanical properties and structure of the epoxy polymers: molecular

- dynamics simulation,” *Journal of Molecular Modeling*, vol. 19, no. 9, pp. 3719–3731, Sep. 2013.
- [12] E. Urbaczewski-Espuche, J. Galy, J.-F. Gerard, J.-P. Pascault, and H. Sautereau, “Influence of chain flexibility and crosslink density on mechanical properties of epoxy/amine networks,” *Polymer engineering & science*, vol. 31, no. 22, pp. 1572–1580, 1991.
- [13] M. K. Umboh, T. Adachi, T. Nemoto, M. Higuchi, and Z. Major, “Non-stoichiometric curing effect on fracture toughness of nanosilica particulate-reinforced epoxy composites,” *Journal of Materials Science*, vol. 49, no. 21, pp. 7454–7461, Nov. 2014.
- [14] T. E. Tay, H. G. Ang, and V. P. W. Shim, “An empirical strain rate-dependent constitutive relationship for glass-fibre reinforced epoxy and pure epoxy,” *Composite Structures*, vol. 33, no. 4, pp. 201–210, Jan. 1995.
- [15] T. Yokoyama, K. Nakai, and N. H. Mohd Yatim, “High Strain-Rate Compressive Stress-Strain Response of Bulk Epoxy Structural Adhesive,” *Journal of Japanese Society for Experimental Mechanics*, vol. 11, no. special issue, pp. 204–209, 2011.
- [16] T. Yokoyama, K. Nakai, and N. H. Mohd Yatim, “High Strain-Rate Compressive Properties and Constitutive Modeling of Bulk Structural Adhesives,” *The Journal of Adhesion*, vol. 88, no. 4–6, pp. 471–486, Apr. 2012.



- [17] H. AL-Zubaidy, X.-L. Zhao, and R. Al-Mihaidi, "Mechanical Behaviour of Normal Modulus Carbon Fibre Reinforced Polymer (CFRP) and Epoxy under Impact Tensile Loads," *Procedia Engineering*, vol. 10, pp. 2453–2458, 2011.
- [18] Z. Jia, D. Hui, G. Yuan, J. Lair, K. Lau, and F. Xu, "Mechanical properties of an epoxy-based adhesive under high strain rate loadings at low temperature environment," *Composites Part B: Engineering*, vol. 105, pp. 132–137, Nov. 2016.
- [19] G. Challita, R. Othman, and K. Khalil, "Compression and shear behavior of epoxy SA 80 bulk adhesive over wide ranges of strain rate," *Journal of Polymer Engineering*, vol. 36, no. 2, Jan. 2016.
- [20] T. Gómez-del Río and J. Rodríguez, "Compression yielding of epoxy: Strain rate and temperature effect," *Mater. Des.*, vol. 35, pp. 369–373, Mar. 2012.
- [21] W. Chen, F. Lu, and M. Cheng, "Tension and compression tests of two polymers under quasi-static and dynamic loading," *Polymer Testing*, vol. 21, no. 2, pp. 113–121, Jan. 2002.
- [22] T. Sugaya, T. Obuchi, and C. Sato, "Influences of Loading Rates on Stress-Strain Relations of Cured Bulks of Brittle and Ductile Adhesives," *Journal of Solid Mechanics and Materials Engineering*, vol. 5, no. 12, pp. 921–928, 2011.

- [23] K. Nakai and T. Yokoyama, “Uniaxial Compressive Response and Constitutive Modeling of Selected Polymers Over a Wide Range of Strain Rates,” *Journal of Dynamic Behavior of Materials*, vol. 1, no. 1, pp. 15–27, Mar. 2015.
- [24] M. D. Banea, S. De, S. Da, R. D. S. G. Campilho, and P. De, “Effects of temperature and loading rate on the mechanical properties of a high temperature epoxy adhesive,” *Journal of Adhesion Science and Technology*, vol. 25, no. 18, pp. 2461–2474, 2011.
- [25] L. Monette, M. P. Anderson, H. D. Wagner, and R. R. Mueller, “The Young’s modulus of silica beads/epoxy composites: Experiments and simulations,” *Journal of Applied Physics*, vol. 75, no. 3, p. 1442, 1994.
- [26] H. Wang, Y. Bai, S. Liu, J. Wu, and C. P. Wong, “Combined effects of silica filler and its interface in epoxy resin,” *Acta Materialia*, vol. 50, no. 17, pp. 4369–4377, 2002.
- [27] M. Conradi, M. Zorko, A. Kocijan, and I. Verpoest, “Mechanical properties of epoxy composites reinforced with a low volume fraction of nanosilica fillers,” *Materials Chemistry and Physics*, vol. 137, no. 3, pp. 910–915, Jan. 2013.
- [28] A. J. Kinloch and A. C. Taylor, “Mechanical and fracture properties of epoxy/inorganic micro-and nano-composites,” *Journal of Materials Science Letters*, vol. 22, no. 20, pp. 1439–1441, 2003.

- [29] T. Adachi, M. Osaki, W. Araki, and S.-C. Kwon, "Fracture toughness of nano- and micro-spherical silica-particle-filled epoxy composites," *Acta Materialia*, vol. 56, no. 9, pp. 2101–2109, May 2008.
- [30] Ibtihal, A. Ibrahim, and M. Hassan, "Study the Mechanical Properties of Epoxy Resin Reinforced With silica (quartz) and Alumina Particles," *The Iraqi Journal For Mechanical And Material Engineering*, vol. 11, no. 3, 2011.
- [31] P. Dittanet and R. A. Pearson, "Effect of bimodal particle size distributions on the toughening mechanisms in silica nanoparticle filled epoxy resin," *Polymer*, vol. 54, no. 7, pp. 1832–1845, Mar. 2013.
- [32] P. Dittanet and R. A. Pearson, "Effect of silica nanoparticle size on toughening mechanisms of filled epoxy," *Polymer*, vol. 53, no. 9, pp. 1890–1905, Apr. 2012.
- [33] A. Jumahat, C. Soutis, F. R. Jones, and A. Hodzic, "Effect of silica nanoparticles on compressive properties of an epoxy polymer," *Journal of Materials Science*, vol. 45, pp. 5973–5983, 2010.
- [34] F. Bondioli, V. Cannillo, E. Fabbri, and M. Messori, "Epoxy-silica nanocomposites: Preparation, experimental characterization, and modeling," *Journal of Applied Polymer Science*, vol. 97, no. 6, pp. 2382–2386, Sep. 2005.

- [35] G. Ragosta, M. Abbate, P. Musto, G. Scarinzi, and L. Mascia, "Epoxy-silica particulate nanocomposites: Chemical interactions, reinforcement and fracture toughness," *Polymer*, vol. 46, no. 23, pp. 10506–10516, Nov. 2005.
- [36] Y. Zheng, K. Chonung, G. Wang, P. Wei, and P. Jiang, "Epoxy/nano-silica composites: Curing kinetics, glass transition temperatures, dielectric, and thermal-mechanical performances," *Journal of Applied Polymer Science*, pp. 917-927, 2008.
- [37] S. Feli and M. M. Jalilian, "Experimental and optimization of mechanical properties of epoxy/nanosilica and hybrid epoxy/fiberglass/nanosilica composites," *Journal of Composite Materials*, Jan. 2016.
- [38] M. H. Kothmann, R. Zeiler, A. Rios de Anda, A. Brückner, and V. Altstädt, "Fatigue crack propagation behaviour of epoxy resins modified with silica-nanoparticles," *Polymer*, vol. 60, pp. 157–163, Mar. 2015.
- [39] S.-Y. Fu, X.-Q. Feng, B. Lauke, and Y.-W. Mai, "Effects of particle size, particle/matrix interface adhesion and particle loading on mechanical properties of particulate-polymer composites," *Composites Part B: Engineering*, vol. 39, no. 6, pp. 933–961, Sep. 2008.
- [40] H. Zhang, L.-C. Tang, Z. Zhang, K. Friedrich, and S. Sprenger, "Fracture behaviours of in situ silica nanoparticle-filled epoxy at different temperatures," *Polymer*, vol. 49, no. 17, pp. 3816–3825, Aug. 2008.

- [41] C. Chen, R. S. Justice, D. W. Schaefer, and J. W. Baur, "Highly dispersed nanosilica–epoxy resins with enhanced mechanical properties," *Polymer*, vol. 49, no. 17, pp. 3805–3815, Aug. 2008.
- [42] M. S. Islam, R. Masoodi, and H. Rostami, "The Effect of Nanoparticles Percentage on Mechanical Behavior of Silica-Epoxy Nanocomposites," *Journal of Nanoscience*, vol. 2013, pp. 1–10, 2013.
- [43] B. B. Johnsen, A. J. Kinloch, R. D. Mohammed, A. C. Taylor, and S. Sprenger, "Toughening mechanisms of nanoparticle-modified epoxy polymers," *Polymer*, vol. 48, no. 2, pp. 530–541, Jan. 2007.
- [44] J. C. H. Affdl and J. L. Kardos, "The Halpin-Tsai equations: A review," *Polymer Engineering and Science*, vol. 16, no. 5, pp. 344–352, May 1976.
- [45] T. B. Lewis and L. E. Nielsen, "Dynamic mechanical properties of particulate-filled composites," *Journal of Applied Polymer Science*, vol. 14, no. 6, pp. 1449–1471, 1970.
- [46] E. H. Kerner, "The Elastic and Thermo-elastic Properties of Composite Media," *Proceedings of the Physical Society. Section B*, vol. 69, no. 8, pp. 808–813, Aug. 1956.
- [47] P. L. Teh, M. Mariatti, A. N. R. Wagiman, and K. S. Beh, "Effect of Curing Agent on the Properties of Mineral Silica Filled Epoxy Composites," *Polymer Composites*, no. 29, pp. 27–36, 2008.

- [48] Y.-G. Miao *et al.*, “Determination of dynamic elastic modulus of polymeric materials using vertical split Hopkinson pressure bar,” *International Journal of Mechanical Sciences*, vol. 108–109, pp. 188–196, Apr. 2016.
- [49] P. Rosso and L. Ye, “Epoxy/Silica Nanocomposites: Nanoparticle-Induced Cure Kinetics and Microstructure,” *Macromolecular Rapid Communications*, vol. 28, no. 1, pp. 121–126, Jan. 2007.
- [50] Y. Hua, L. Gu, S. Premaraj, and X. Zhang, “Role of Interphase in the Mechanical Behavior of Silica/Epoxy Resin Nanocomposites,” *Materials*, vol. 8, no. 6, pp. 3519–3531, Jun. 2015.
- [51] M. Imanaka, Y. Takeuchi, Y. Nakamura, A. Nishimura, and T. Iida, “Fracture toughness of spherical silica-filled epoxy adhesives,” *International journal of adhesion and adhesives*, vol. 21, no. 5, pp. 389–396, 2001.
- [52] T. H. Hsieh, A. J. Kinloch, K. Masania, A. C. Taylor, and S. Sprenger, “The mechanisms and mechanics of the toughening of epoxy polymers modified with silica nanoparticles,” *Polymer*, vol. 51, no. 26, pp. 6284–6294, Dec. 2010.
- [53] Y. Zare, “A simple technique for determination of interphase properties in polymer nanocomposites reinforced with spherical nanoparticles,” *Polymer*, vol. 72, pp. 93–97, Aug. 2015.

- [54] Y. Zare and H. Garmabi, "A developed model to assume the interphase properties in a ternary polymer nanocomposite reinforced with two nanofillers," *Composites Part B: Engineering*, vol. 75, pp. 29–35, Jun. 2015.
- [55] T. Ahmad, O. Mamat, and R. Ahmad, "Studying the Effects of Adding Silica Sand Nanoparticles on Epoxy Based Composites," *Journal of Nanoparticles*, vol. 2013, pp.1-5, Jan. 2013.
- [56] E. Bugnicourt, J. Galy, J.-F. Gérard, and H. Barthel, "Effect of sub-micron silica fillers on the mechanical performances of epoxy-based composites," *Polymer*, vol. 48, no. 6, pp. 1596–1605, Mar. 2007.
- [57] P. Cassagnau, "Melt rheology of organoclay and fumed silica nanocomposites," *Polymer*, vol. 49, no. 9, pp. 2183–2196, Apr. 2008.
- [58] M. Pishvaei, P. Cassagnau, and T. F. McKenna, "Modelling of The Rheological Properties of Bimodal Emulsions," *Macromolecular Symposia*, vol. 243, no. 1, pp. 63–71, Nov. 2006.
- [59] S. Kang, S. I. Hong, C. R. Choe, M. Park, S. Rim, and J. Kim, "Preparation and characterization of epoxy composites filled with functionalized nanosilica particles obtained via sol–gel process," *Polymer*, vol. 42, no. 3, pp. 879–887, 2001.

- [60] C. Chen and A. B. Morgan, "Mild processing and characterization of silica epoxy hybrid nanocomposite," *Polymer*, vol. 50, no. 26, pp. 6265–6273, Dec. 2009.
- [61] B. Fiedler, F. H. Gojny, M. H. G. Wichmann, M. C. M. Nolte, and K. Schulte, "Fundamental aspects of nano-reinforced composites," *Composites Science and Technology*, vol. 66, no. 16, pp. 3115–3125, Dec. 2006.
- [62] R. Greenwood, P. F. Luckham, and T. Gregory, "The Effect of Diameter Ratio and Volume Ratio on the Viscosity of Bimodal Suspensions of Polymer Latices," *Journal of Colloid and Interface Science*, vol. 191, no. 1, pp. 11–21, Jul. 1997.
- [63] R. Greenwood, P. F. Luckham, and T. Gregory, "Minimising the viscosity of concentrated dispersions by using bimodal particle size distributions," *Colloids and Surfaces A: Physicochemical and Engineering Aspects*, vol. 144, no. 1, pp. 139–147, 1998.
- [64] B. Dames, B. R. Morrison, and N. Willenbacher, "An empirical model predicting the viscosity of highly concentrated, bimodal dispersions with colloidal interactions," *Rheologica Acta*, vol. 40, no. 5, pp. 434–440, 2001.
- [65] S.-C. Kwon, T. Adachi, W. Araki, and A. Yamaji, "Effect of composing particles of two sizes on mechanical properties of spherical silica-particulate-reinforced epoxy composites," *Composites Part B: Engineering*, vol. 39, no. 4, pp. 740–746, Jun. 2008.



- [66] M. Shariati, G. A. Farzi, A. Dadrasi, M. Amiri, and R. Rashidi Meybodi, "An Experimental Study on Toughening Mechanisms of Fillers in Epoxy/Silica Nanocomposites," *International Journal of Nanoscience and Nanotechnology*, vol. 11, no. 3, pp. 193–199, 2015.
- [67] M. Keivani, A. Khamesinia, R. Bagheri, M. A. Kouchakzadeh, and M. Abadyan, "Study of synergistic toughening in a bimodal epoxy nanocomposite," *Journal of Reinforced Plastics and Composites*, vol. 34, no. 4, pp. 281–292, Feb. 2015.
- [68] A. Dorigato, Y. Dzenis, and A. Pegoretti, "Filler aggregation as a reinforcement mechanism in polymer nanocomposites," *Mechanics of Materials*, vol. 61, pp. 79–90, Jul. 2013.
- [69] Y. A. Dzenis, "Effect of aggregation of a dispersed rigid filler on the elastic characteristics of a polymer composite," *Mechanics of Composite Materials*, vol. 22, no. 1, pp. 12–19, 1986.
- [70] S. Gunawan and R. Gibson, "Analytical and experimental characterization of extensional damping in single lap viscoelastic adhesive joints," in *28th Structures, Structural Dynamics and Materials Conference*, American Institute of Aeronautics and Astronautics.
- [71] S.-W. Koh, J.-K. Kim, and Y.-W. Mai, "Fracture toughness and failure mechanisms in silica-filled epoxy resin composites: effects of temperature and loading rate," *Polymer*, vol. 34, no. 16, pp. 3446–3455, 1993.

- [72] Y. Tian *et al.*, “High strain rate compression of epoxy based nanocomposites,” *Composites Part A: Applied Science and Manufacturing*, vol. 90, pp. 62–70, Nov. 2016.
- [73] A. T. Owens and H. V. Tippur, “A Tensile Split Hopkinson Bar for Testing Particulate Polymer Composites Under Elevated Rates of Loading,” *International Journal of Fracture*, vol. 49, no. 6, pp. 799–811, Dec. 2009.
- [74] S.-C. Kwon, T. Adachi, and W. Araki, “Temperature dependence of fracture toughness of silica/epoxy composites: Related to microstructure of nano- and micro-particles packing,” *Composites Part B: Engineering*, vol. 39, no. 5, pp. 773–781, Jul. 2008.
- [75] S. Sprenger, “Epoxy resins modified with elastomers and surface-modified silica nanoparticles,” *Polymer*, vol. 54, no. 18, pp. 4790–4797, Aug. 2013.
- [76] M. Zamanian, M. Mortezaei, B. Salehnia, and J. E. Jam, “Fracture toughness of epoxy polymer modified with nanosilica particles: Particle size effect,” *Engineering Fracture Mechanics*, vol. 97, pp. 193–206, Jan. 2013.
- [77] J.-L. Tsai, H. Hsiao, and Y.-L. Cheng, “Investigating Mechanical Behaviors of Silica Nanoparticle Reinforced Composites,” *Journal of Composite Materials*, vol. 44, no. 4, pp. 505–524, Feb. 2010.

- [78] Y. Zare, “Study of nanoparticles aggregation/agglomeration in polymer particulate nanocomposites by mechanical properties,” *Composites Part A: Applied Science and Manufacturing*, vol. 84, pp. 158–164, May 2016.
- [79] T. Adachi, W. Araki, and M. Higuchi, “Mixture law including particle-size effect on fracture toughness of nano- and micro-spherical particle-filled composites,” *Acta Mechanica*, vol. 214, no. 1–2, pp. 61–69, Oct. 2010.
- [80] Y. Guo and Y. Li, “Quasi-static/dynamic response of SiO<sub>2</sub>–epoxy nanocomposites,” *Materials Science and Engineering: A*, vol. 458, no. 1–2, pp. 330–335, Jun. 2007.
- [81] L. Goglio, L. Peroni, M. Peroni, and M. Rossetto, “High strain-rate compression and tension behaviour of an epoxy bi-component adhesive,” *International Journal of Adhesion and Adhesives*, vol. 28, no. 7, pp. 329–339, Oct. 2008.
- [82] N. K. Naik, P. J. Shankar, V. R. Kavala, G. Ravikumar, J. R. Pothnis, and H. Arya, “High strain rate mechanical behavior of epoxy under compressive loading: Experimental and modeling studies,” *Materials Science and Engineering: A*, vol. 528, no. 3, pp. 846–854, Jan. 2011.
- [83] S. Chaudhary, N. Iqbal, V. Mangla, D. Kumar, and P. K. Roy, “Strain rate sensitivity of toughened epoxy,” *Iranian Polymer Journal*, vol. 24, no. 10, pp. 871–881, Oct. 2015.

- [84] P. Ma, G. Jiang, Y. Li, and W. Zhong, "The Impact Compression Behaviors of Silica Nanoparticles—Epoxy Composites," *Journal of Textile Science and Technology*, vol. 01, no. 01, pp. 1–11, 2015.
- [85] M. F. Omar, H. M. Akil, and Z. A. Ahmad, "Particle size – Dependent on the static and dynamic compression properties of polypropylene/silica composites," *Materials & Design*, vol. 45, pp. 539–547, Mar. 2013.
- [86] H. Zhao and G. Gary, "On the use of SHPB techniques to determine the dynamic behavior of materials in the range of small strains," *International Journal of Solids and structures*, vol. 33, no. 23, pp. 3363–3375, 1996.
- [87] C. Kanchanomai, S. Rattananon, and M. Soni, "Effects of loading rate on fracture behavior and mechanism of thermoset epoxy resin," *Polymer Testing*, vol. 24, no. 7, pp. 886–892, Oct. 2005.
- [88] B. T. Marouf, Y.-W. Mai, R. Bagheri, and R. A. Pearson, "Toughening of Epoxy Nanocomposites: Nano and Hybrid Effects," *Polymer Reviews*, vol. 56, no. 1, pp. 70–112, Jan. 2016.
- [89] P. He, M. Huang, B. Yu, S. Sprenger, and J. Yang, "Effects of nano-silica contents on the properties of epoxy nanocomposites and Ti-epoxy assemblies," *Composites Science and Technology*, vol. 129, pp. 46–52, Jun. 2016.
- [90] Y. Rostamiyan, A. Fereidoon, A. Ghasemi Ghalebahman, A. Hamed Mashhadzadeh, and A. Salmankhani, "Experimental study and optimization

of damping properties of epoxy-based nanocomposite: Effect of using nanosilica and high-impact polystyrene by mixture design approach,” *Material Design 1980-2015*, vol. 65, pp. 1236–1244, Jan. 2015.

- [91] T. Adachi, Y. Imai, and M. Higuchi, “Fracture Energy of Nano-and micro-silica particle-filled epoxy Composites,” *International Journal of Theoretical and Applied Multiscale Mechanics*, vol. 2, no. 1, pp. 82–94, 2011.
- [92] R. Greenwood, P. F. Luckham, and T. Gregory, “Minimising the viscosity of concentrated dispersions by using bimodal particle size distributions,” *Colloids and Surfaces A: Physicochemical and Engineering Aspects*, vol. 144, no. 1, pp. 139–147, 1998.
- [93] S. C. Kwon, T. Adachi, W. Araki, and A. Yamaji, “Effect of Particle Size on Fracture Toughness of Spherical-Silica Particle Filled Epoxy Composites,” *Key Engineering Materials*, vol. 297–300, pp. 207–212, 2005.
- [94] P. Dittanet and R. A. Pearson, “Effect of bimodal particle size distributions on the toughening mechanisms in silica nanoparticle filled epoxy resin,” *Polymer*, vol. 54, no. 7, pp. 1832–1845, Mar. 2013.
- [95] T. J. Cloete, G. Paul, and E. B. Ismail, “Hopkinson bar techniques for the intermediate strain rate testing of bovine cortical bone,” *Philosophical*

*Transactions of the Royal Society A: Mathematical, Physical and Engineering Sciences*, vol. 372, no. 2015, pp. 1–13, May 2014.

- [96] A. Caverzan, E. Cadoni, and M. di Prisco, “Tensile behaviour of high performance fibre-reinforced cementitious composites at high strain rates,” *International Journal of Impact Engineering*, vol. 45, pp. 28–38, Jul. 2012.
- [97] A. Gilat, R. K. Goldberg, and G. D. Roberts, “Experimental study of strain-rate-dependent behavior of carbon/epoxy composite,” *Composites Science and Technology*, vol. 62, no. 10–11, pp. 1469–1476, Aug. 2002.
- [98] W. Chen, B. Zhang, and M. J. Forrester, “A split Hopkinson bar technique for low-impedance materials,” *Experimental mechanics*, vol. 39, no. 2, pp. 81–85, 1999.
- [99] F. Dai, K. Xia, and S. N. Luo, “Semicircular bend testing with split Hopkinson pressure bar for measuring dynamic tensile strength of brittle solids,” *Review of Scientific Instruments*, vol. 79, no. 12, p. 123903, Dec. 2008.
- [100] D. J. Frew, M. J. Forrester, and W. Chen, “A split Hopkinson pressure bar technique to determine compressive stress-strain data for rock materials,” *Experimental mechanics*, vol. 41, no. 1, pp. 40–46, 2001.
- [101] D. J. Frew, “Pulse Shaping Techniques for Testing Elastic-plastic Materials with a Split Hopkinson Pressure Bar,” *Experimental mechanics*, vol. 45, no. 2, pp. 186–195, Apr. 2005.

- [102] Y. Goda and T. Sawa, “Study on the effect of strain rate of adhesive material on the stress state in adhesive joints,” *Journal of Adhesion*, vol. 87, no. 7–8, pp. 766–779, 2011.
- [103] H. Zhao and G. Gary, “On the use of SHPB techniques to determine the dynamic behavior of materials in the range of small strains,” *International Journal of Solids and structures*, vol. 33, no. 23, pp. 3363–3375, 1996.
- [104] A. Bekker, T. J. Cloete, A. Chinsamy-Turan, G. N. Nurick, and S. Kok, “Constant strain rate compression of bovine cortical bone on the Split-Hopkinson Pressure Bar,” *Materials Science and Engineering: C*, vol. 46, pp. 443–449, Jan. 2015.
- [105] W. Chen, B. Song, D. J. Frew, and M. J. Forrester, “Dynamic small strain measurements of a metal specimen with a split Hopkinson pressure bar,” *Experimental Mechanics*, vol. 43, no. 1, pp. 20–23, Mar. 2003.
- [106] B. Song, “Loading and Unloading Split Hopkinson Pressure Bar Pulse-shaping Techniques for Dynamic Hysteretic Loops,” *Experimental Mechanics*, vol. 44, no. 6, pp. 622–627, Dec. 2004.
- [107] B. Song and W. Chen, “Loading and unloading split hopkinson pressure bar pulse-shaping techniques for dynamic hysteretic loops,” *Experimental Mechanics*, vol. 44, no. 6, pp. 622–627, Dec. 2004.

- [108] S. . Olhero and J. M. . Ferreira, “Influence of particle size distribution on rheology and particle packing of silica-based suspensions,” *Powder Technology*, vol. 139, no. 1, pp. 69–75, Jan. 2004.
- [109] J. Tarrío-Saavedra, “Controversial effects of fumed silica on the curing and thermomechanical properties of epoxy composites,” *Express Polymer Letters*, vol. 4, no. 6, pp. 382–395, May 2010.
- [110] R. Yang, Y. Song, and Q. Zheng, “Payne effect of silica-filled styrene-butadiene rubber,” *Polymer*, vol. 116, pp. 304–313, May 2017.
- [111] L. Sun, R. F. Gibson, F. Gordaninejad, and J. Suhr, “Energy absorption capability of nanocomposites: A review,” *Composites Science and Technology*, vol. 69, no. 14, pp. 2392–2409, Nov. 2009.
- [112] A. Kara, A. Tasdemirci, and M. Guden, “Modeling quasi-static and high strain rate deformation and failure behavior of a ( $\pm 45$ ) symmetric E-glass/polyester composite under compressive loading,” *Materials & Design*, vol. 49, pp. 566–574, Aug. 2013.
- [113] B. Song, W. Chen, T. Yanagita, and D. J. Frew, “Confinement effects on the dynamic compressive properties of an epoxy syntactic foam,” *Composite Structures*, vol. 67, no. 3, pp. 279–287, Mar. 2005.
- [114] D. Kroisová, “An internal damping in epoxy composite systems,” *Proceeding of ISMA (International Conference on Vibration and Noise Engineering)*, vol. 30, Sep. 2010.



## List of Publications

1. Yohanes and Y. Sekiguchi, "Influence of Mixed Micro and Nano Silica Fillers on Dynamic Stiffness of Epoxy Adhesive", *Proceedings ACA (Asian Conference on Adhesion)*, vol.6, pp.47-48, June 2016.
2. Yohanes and Y. Sekiguchi, "Effects of mixed micro and nano silica particles on the dynamic compressive performances of epoxy adhesive," *Applied Adhesion Science*, vol. 5, no. 1, pp.3-14, Feb. 2017.
3. Yohanes and Y. Sekiguchi, "Synergistic Effects of Mixed Silica Micro-nanoparticles on Compressive Dynamic Stiffness and Damping of Epoxy Adhesive," *Journal of Dynamic Behavior of Materials*, vol. 4, no. 2, pp. 190-200, Mar. 2018.

## Acknowledgments

I sincerely appreciate Assoc. Prof. Yasuhisa Sekiguchi for his encouragement, supervision, and support from the very beginning to the concluding level of my doctorate study. All achievements in this study would not have been possible without his great support.

I also acknowledge the members of my dissertation committee, Prof. Ryo Kikuuwe, Prof. Soichi Ibaraki, and Assoc. Prof. Ryuutarou Hino for giving their generously time and expertise to improve my work. I sincerely thank them for their helpful suggestions, insightful discussions, and their good-natured support.

I would also like to thank my family and friends, especially Mr. Arlyn, Mr. Dwitama, Mr. Irwan, and Mr. Zuhaj, who supported me in any respect during the completion of this study. I also would like to thank all staff of the graduate school of engineering at Hiroshima University for all the help and support.